Dimensioning of large chimneys

Written by

Marcus Nilsson

Martin Johansson

ISRN LUTFD2/TFME—08/5005—SE(1-62)

Preface

This master's thesis has been written at the Division of Mechanics at Lund's Institute of Technology in cooperation with Epsilon High Tech/Technology in Malmoe during the fall and winter 2007-2008. The purpose of the work was to create a construction manual, guiding the designers at Gullmanders Arking AB when designing chimneys.

We would like to thank our supervisors, Professor Solveig Melin and Nic Gullmander for their great support and handling. Also a great thanks to the management of the High Tech group regarding support and equipment needed for this project.

A special thank to Gullmanders Arking AB and Källreda Plåt och Smides AB for their support and hospitality when visiting.

Regards,

Marcus Nilsson
Martin Johansson

Abstract

This master's thesis was written in cooperation with Epsilon High Tech/Technology in Malmoe and concerns analysis of the lower part of large chimney exposed to different kinds of wind load. These chimneys are manufactured by Källreda Plåt och Smides AB after being dimensioned by Gullmanders Arking AB.

The main objective was to analyse the lower part of the chimney, including the sheet metal supports and guide rings, in order to try to find relations between the parts and create a construction manual to guide the designers at Gullmanders Arking AB when dimensioning. Due to the large variety of chimneys, some kind of standardization was called for so that the manufacturing cost could be reduced. This involves cutting down on the thicknesses and the number of detailed parts of the lower part of the chimney.

When dimensioning, not only static loading was considered, but also the risk of occurance of phenomena's like fatigue and buckling were evaluated. The common dimensioning criterion when analysing both static and dynamic loadings was that no yielding was allowed. The buckling analysis included the sheet metal supports while all detailed parts were considered when performing the fatigue analysis. The loading on the structure was determined according to the norms in the Snö och Vindlast (BSV97) in the so-called wind exposure analysis. The strength of the structure was, however, determined using the norms of BSK99.

The chimney was modelled and analyzed by using the commercial Finite Element solver ABAQUS. Due to the large number of different sizes of chimneys, a parameterisation was imposed. By writing a Python script, chimneys with different sizes and number of details could easy be modelled.

In the analytical calculations made by Gullmanders Arking AB, the thickness of the sheet metals supports was set to be 12 mm. The buckling analysis showed that there was no sign of the mentioned phenomenon appearing at the given thickness. Therefore the thickness was reduced to 8 mm, which also fulfilled the fatigue criterion. Further, the guide rings were given constant thicknesses. It could be seen from the strength analysis that the top guide ring never was close to failure and was, therefore, standardized to 10 mm. The bottom guide ring was, however, heavily loaded due to the mounting, and the number of sheet metal supports were of great importance when considering the yield criterion. The thickness of the bottom guide ring was set to 20 mm and the number of sheet metal supports was increased to strengthen the guide ring, if needed. The structure was analyzed to the point of where failure of the casing appeared. At this point it did not matter if the lower part of the chimney was stiffened.

Sammanfattning

Detta examensarbete har skrivits i samarbete med Epsilon High Tech/Technology i Malmö. Syftet var att analysera den nedre delen av en skorsten utsatt för olika former av vindlast. Skorstenarna är tillverkade av Källreda Plåt och Smides AB och dimensionerade av Gullmanders Arking AB.

Uppgiften var att analysera den nedre delen av skorstenen, inkluderande stödplåtar och flänsringar, för att försöka hitta relationer mellan delarna och skapa en konstruktionsmanual som hjälper konstruktörerna på Gullmanders Arking AB vid dimensionering. På grund av den stora antalet olika skorstenar, var någon form av standardisering nödvändig syftande till att reducera produktionskostnaderna. Detta innebär en minskning av både plåttjocklek och antalet ingående delar hos den nedre delen av skorstenen.

När man dimensionerar en skorsten förutsätts dess ingående delar inte bara klara av den statiska last som den är utsatt för, d v s inte uppvisa flytning, utan även risken för utmattning måste utvärderas. Stödplåtarna måste förutom de nyss nämnda dimensioneringskraven även utvärderas mot buckling. Då belastningssituationen är komplex bestäms lasterna genom en vindanalys styrd av normhandboken Snö och Vindlast (BSV97). Hållfastheten hos konstruktionen beräknas med hjälp av normhandboken BSK99.

Skorsten modellerades och analyserades i det kommersiella finita element programmet ABAQUS. Då ett stort antal skorstenar med olika geometri skulle analyseras skrevs ett skript som utförde modelleringen med ett givet antal olika geometriska parametrar.

Genom handberäkningarna, genomförda av Gullmanders Arking AB, var tjockleken på stödplåtarna satt till 12 mm. Bucklingsanalysen visade dock inga tecken på buckling, vilket var det som plåtarna dimensionerades mot. Detta innebar att tjockleken kunde sättas till 8 mm. Det visade sig att med denna tjocklek skulle skorstenen även klara av utmattningskriteriet. Vidare var flänsringarna givna konstanta tjocklekar. Hållfasthetsanalyserna visade att den övre flänsringen, som var given en tjocklek på 10 mm, aldrig skulle bli dimensionerande för skorstenens funktion. Undre flänsringen, däremot, var ofta tungt belastad på grund av förankringen, och antalet stödplåtar var av största betydelse vid dimensionering mot flytvillkoret. Tjockleken av undre flänsring sattes till 20 mm och istället ökades, om möjligt, antalet stödplåtar för att styrka flänsringen. Det visade sig att en dimensioneringsgräns uppnåddes då en ökning av antalet plåtar ej påverkade konstruktionen, nämligen då manteln blev dimensionerande.

Table of contents

1 Introduction

1.1 Background

Chimneys are very common constructions at industries. Even if they may look simple, they are not trivial to dimension. The slender shape makes them extremely vulnerable to loadings, such as wind exposure. They are therefore very interesting objects to analyze.

The Swedish company Källreda Plåt- & Smides AB has over 35 years experience of manufacturing chimneys. With the ability of fully customizing the chimneys on the basis of the customers needs, and with a total number of 1800 delivered chimneys, they are today one of Sweden's largest and most experienced chimney manufacturers.

The dimensioning was, from the beginning and still is, provided by Gullmanders Arking AB in Lenhovda. By using simplified analytical calculations in accordance with pertinent norms they are today guaranteeing the safety of the chimneys built.

Due to the present high prices of steel, Källreda Plåt- & Smides AB is very concerned with optimizing the geometry of the construction. The intuitive feeling is that some of the approximations performed in the analytical solutions lead to a conservative result and, thereby, to an unnecessarily rough structure.

Therefore a request was sent by Gullmanders Arking AB to Epsilon Technology/High Tech with the purpose of investigating these issues and, preferably, to come up with improvements of the construction.

1.2 The Geometry

The rather complex construction is actually built up by a number of relatively non-complex parts. The chimney is mounted to the ground by a specially built foundation. The different parts may be seen in Figure 1-1.

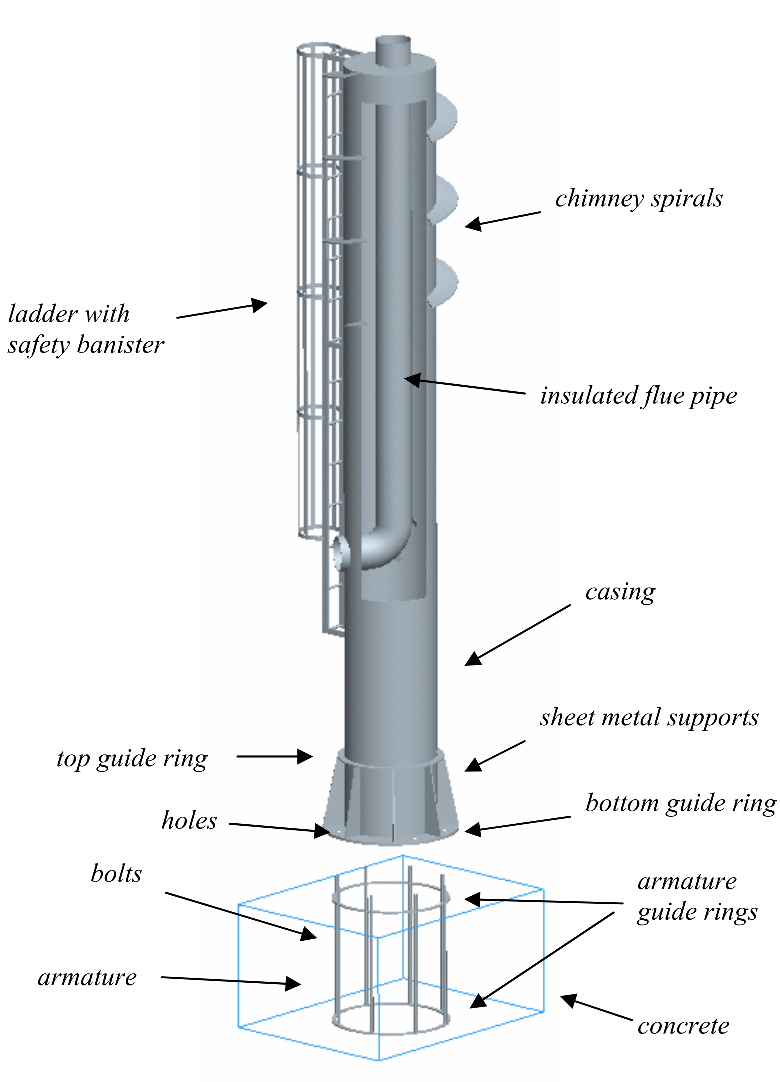

Figure 1-1. *The chimney with its parts.*

The main part of the chimney is the casing. It is the centre that connects all parts finally constituting the chimney at the same time as it is supposed to maintain the strength and stability of the structure.

When manufacturing the casing, metal sheets are bent into circular sections with a height of 1.5 meters and desired diameter. These sections are then welded together to form the tube which establishes the casing. The thickness of each section is varying and is determined by the wind exposure analysis.

The height of the casing is depending on circumstances such as where the chimney will be mounted geographically, and of what chemical substances it is meant to lead. If unhealthy substances in the flues are lead out, or if the chimney is supposed to be mounted in crowded areas, the diffusion must be high enough to guarantee human and environmental health. Tougher demands lead, of course, to that a higher casing is needed.

The casing diameter depends on both the sizes and the number of insulated flue pipes that runs inside of the casing and on restrictions put on the slenderness. The largest aspect ratio, i.e. height vs. diameter, that may be used, is set to 40. This may lead to that a larger diameter than actually needed must be used.

The ladder with its safety banister, which for example is used for inspections, is, in most cases, connected to the outside of the casing, but, sometimes, to the inside, when possible.

Chimney spirals are, when needed, welded to the top of the casing in order to decrease the effects of the so-called vortex shedding phenomena.

To securely mount the chimney to the foundation, a bottom guide ring is welded to the base of the casing. To increase stability, a top guide ring is welded above this guide ring. Between these are a number of sheet metal supports added in order to distribute the local forces around the base of the chimney.

Holes are made in the bottom guide ring so that the structure may be bolted onto the foundation. These holes are drilled with equal distances in the centre of the bottom guide ring, between the sheet metal supports.

This foundation consists of an armature containing threaded bolts, fixed together via the armature guide rings. This armature is then concreted onto the ground in order to create maximum stability.

The mounting procedure is quite complex and is therefore explained in detail later, but the major effect of it is that it leaves the bolts with a pretension.

1.3 The Wind Exposure analysis

When dimensioning chimneys, the major loading consists of the exposure of winds. The wind is, by nature, dynamic, but it may be separated into one static and one dynamic part of loading. The dynamic part leads to fatigue failure of the construction whereas the static part may lead to collapse in terms of buckling or fracture failure.

Wind based calculations are often very complex, with a lot of parameters affecting the result. Not only geometrical and geographical circumstances must be evaluated, but also statistics must be used due to the randomness of the wind. The calculations are therefore performed according to the norms in Snö och Vindlast (BSV97). The theories behind these norms are only presented here, but the calculations are excluded due to their complexity. The main thing is, however, the results from the calculations, which are used as an input to this Master's thesis. More about this is explained later.

Worth knowing about wind exposure is that it may be divided into three categories. One that covers the usual behaviour of the wind exposure, i.e. the static wind load, one that covers suddenly occurring wind increments, i.e. wind gusts, and, finally, one that considers the phenomenon of vortex shedding that appears during wind moves around obstacles. As opposed to the wind gust the vortex shedding leads to oscillations of the chimney perpendicular to the wind direction. This phenomenon may be seen if observing flagpoles during windy days. In Figure 1-2 the three wind exposures are illustrated.

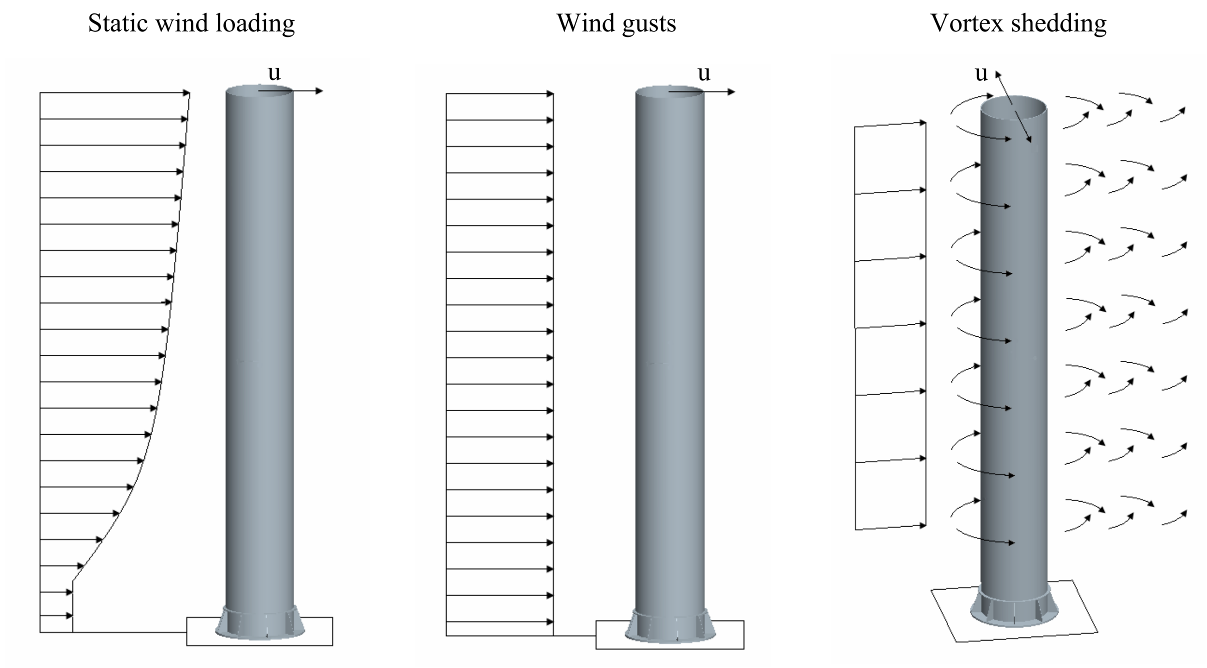

Figure 1-2. *Three types of wind loading with respective deflections.*

2 Objective

As previously mentioned, improvements are believed to be possible at dimensioning considering the simplifications during analytical dimensioning of the chimneys.

The main objective of this Master’s thesis is to concentrate on, and to analyze, the lower part of the chimney, including the sheet metal supports and guide rings, in order to try to find relations between the parts and to create a construction manual to guide the designers at Gullmanders Arking AB.

The main thing is to try to standardize the number of components and their thicknesses as regard the sheet metal supports, and to standardize the thicknesses of the top and bottom guide rings.

Due to the large variety of chimneys, a standardization of the included parts is, if possible, required for the chimneys with the diameters and parameters given in Table 2-1.

Table 2-1. *Parameters sought for in defining diameters of the casings.*

Casing diameter (mm)	Number of sheet metal supports	Thickness of sheet metal supports	Thickness of top guide ring	Thickness of bottom guide ring
D-500	-	-	-	-
D-750	-	-	-	-
D-1000	-	-	-	-
D-1250	-	-	-	-
D-1500	-	-	-	-
D-1750	-	-	-	-
D-2000	-	-	-	-

The calculations and evaluations are to be performed by using the finite element method and the commercial finite element solver ABAQUS.

3 Preliminaries

The concept for building chimneys are quite complex and must therefore be clearly understood. Many parameters are affecting the structure. The parameters may be either geometrical or material specific, or be dependent on the loading. The parameters must either be defined or relations between them found and, in some cases, restrictions are put on the variances of them. The common thing is, though, that all parameters must be regarded by creating a geometry that fulfils all loading criteria. In this chapter the most important parameters are investigated and the most important relations explained, all relating to the lower part of the chimney. The outcome, i.e. the expected result of this Master's thesis, is also discussed.

3.1 The Geometry

As mentioned, all parts are defined by their geometry. The geometrical parameters relating to the lower parts of the chimney are shown in the cross section view in Figure 3-1.

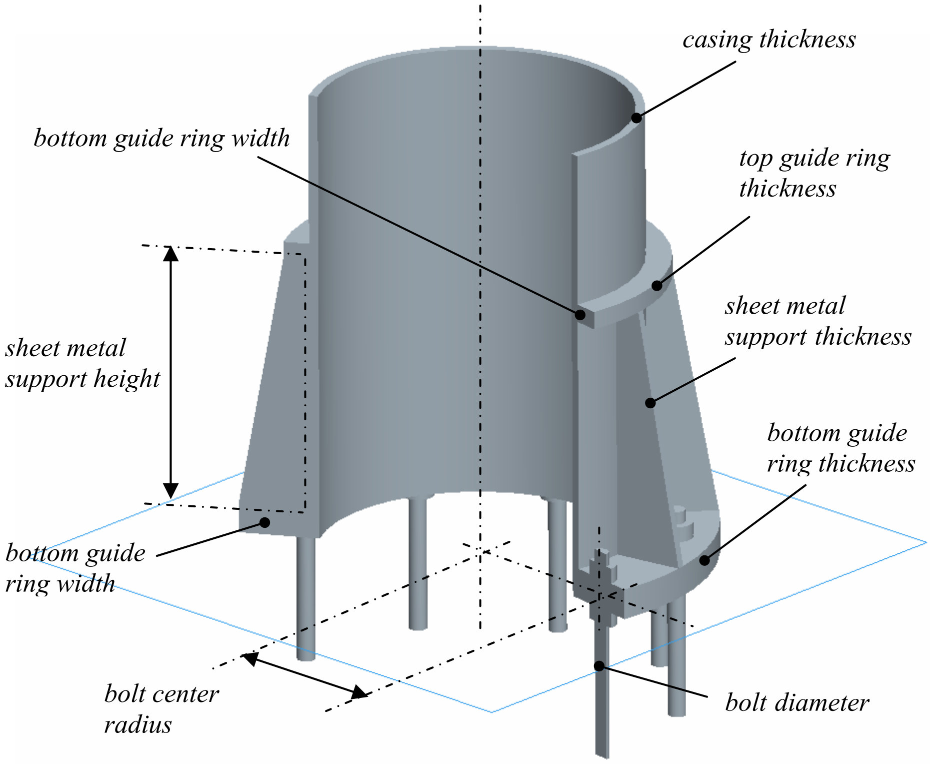

Figure 3-1. *Geometric parameters of the lower part of the chimney.*

Some of the geometric parameters are defined by restrictions, similar to the earlier discussion concerning the height of the casing, which was depending on the diffusion of the flue. Others need to be determined by calculations, while the rest should be defined, only.

In table Table 3-1 the geometric parameters of the geometry in Figure 1-1 are given. The parameters are separated into two columns; one that presents the value of the parameters set fixed and one that presents the parameters that must be determined by calculations.

Table 3-1. *Parameters associated with the lower chimney parts.*

Dimension		Fixed parameters	Calculated parameters
Casing thickness	t_{casing}		6-12 mm
Bolt diameter	D_{bolt}	M24	
Bolt center diameter	$D_{bolt\ center\ diameter}$	Origo - middle of bottom guide ring	
Top guide ring width	$W_{top\ guide\ ring}$	50 mm	
Top guide ring thickness	$t_{top\ guide\ ring}$		10 mm
Bottom guide ring width	$W_{bottom\ guide\ ring}$	150 mm	
Bottom guide ring thickness	$t_{bottom\ guide\ ring}$		20 mm
Sheet metal support height	$h_{sheet\ metal\ support}$	0.5 m	
Sheet metal support thickness	$t_{sheet\ metal\ support}$		12 mm

The thickness of the base section is actually determined by the calculations from the wind exposure analysis and is therefore not presented here. Worth knowing is, however, that the thickness is restricted to never be less than 6 mm, even if a thinner casing would maintain the hypothetical loading. The thickness might however be increased, if needed, in steps of 2 mm up to a casing thickness of 12 mm.

The thickness of the sheet metal supports and the guide rings are given by simple analytical calculations, while the width of the parts is set fixed.

Guidelines are used when choosing the number of sheet metal supports, with holes for the bolts usually drilled in the centre of the lower guide ring. If the distance between the holes is less than 180 mm, there is not enough space to apply the bolt pretension with the torque wrench due to the small spacing between the sheet metal supports, see Figure 3-2.

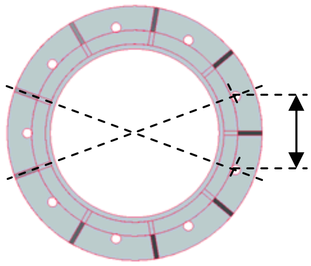

Figure 3-2. *Distance between the holes.*

On the other hand, if this distance is too large, the structure might not manage to withstand the intended loading. Independently of the diameter of the casing, 12 is the minimum number of sheet metal supports used. Using fewer will lead to a lack of bolts to impose the intended pretension.

By experience from earlier built chimneys in combination with the previously mentioned guidelines, the number of sheet metal supports to be evaluated in this Master's thesis is given in Table 3-2.

Table 3-2. *Number of sheet metal supports.*

Diameter (mm)	Number of sheet metal supports
D-500	12-20
D-750	12-24
D-1000	12-24
D-1250	14-26
D-1500	18-30
D-1750	20-36
D-2000	22-38

3.2 Material

A material called CorTen is used in the casing, guide rings and sheet metal supports. CorTen is a relatively strong steel, but its mayor quality is that it is very corrosion resistant. The bolts are made of a high strength steel, SS 2134.

For calculations, parameters like the Young's modulus, Poison's ratio and the yield strength are of great importance. Also the general behaviour of the material is of importance. Some materials might have different properties in different directions which make them more difficult to model, but the steel used here is, fortunately, isotropic.

The material parameters for the given materials may be seen in Table 3-3.

Table 3-3. *Material parameters.*

Parameter	CorTen	SS2134
Young’s modulus	206 GPa	206 GPa
Poison’s ratio	0.3	0.3
Yield strength	340 MPa	340 MPa

3.3 Wind exposure analysis

As mentioned, wind exposure analysis is very complex. The principles may, however, be explained by a simple example. If considering a cantilever beam exposed to a distributed load *q(x)* representing, for example, a wind gust, the moment *M* and the shear force *T* acting over the cross section may easily be analytically calculated by the equilibrium equations given by the Euler-Bernoulli beam theory, see Figure 3-3.

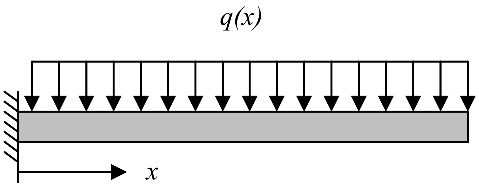

$$\frac{dT(x)}{dx} = q(x)$$
$$\frac{dM(x)}{dx} = T(x)$$

Figure 3-3. *The equilibrium equations giving the shear force T and moment M on a cantilever beam exposed to a distributed load q(x).*

In reality the situation is more complex due to that the dynamics must be considered, and because the behaviour of the wind is arbitrary. Therefore the analysis is performed using the guidelines of the norms in Snö och Vindlast (BSV97). The output of the analysis is the same as for the cantilever beam, the shear force $T_{X=0}$ and the momentum $M_{X=0}$, where the coordinate *x* is defined in Figure 3-3. In this master's thesis, the response of the loading is investigated whereas the source of it is of no interest.

Table 3-4 shows the dimensions and loading data from six recently built chimneys.

Table 3-4. *Data from existing chimneys.*

Dimensions			Axial Force	Static		Wind gust		Whirlwinds	
Diam. (m)	Height (m)	Base section casing thickness (mm)	N (kN)	M (kNm)	T (kN)	M (kNm)	T (kN)	M (kNm)	T (kN)
0.54	20	6	23	178.5	15.5	218.8	19	11.5	1.1
0.63	20	6	26	135	12	170	15	31	3
0.95	27	6	57	378	22	462	27	97	7
1.25	36	6	102	980	41	1171	49	165	10
1.44	52,4	12	221	4218	141	4808	159	211	8
2.1	48	10	207	3101	97	3476	109	759	32

The axial force *N* is representing the weight of the construction, while the moment *M* and the shear force *T* are the previously mentioned loading parameters given by the wind exposure analysis.

The data in Table 3-4 is used when trying to find relations between the dimensions and the loading parameters. The first impression is that the size of the casing is the main parameter that affects the loading parameters. The smaller the chimney is, the smaller the cross section forces are. The chimney spirals also have a significant effect on the load. The spirals increase both the static load and the wind gust load due to the increase in the projected area perpendicular to the wind direction. The profit is, however, the decrease in the vortex shedding effects.

Also worth noticing is that the strength against dynamic loading is strongly dependent on the lifetime of the chimney, which usually is set to 30 years. The lifetime prescribes the number of cycles allowed when dimensioning against fatigue. The wind gust usually appears 60000 times while the whirlwinds appear 10^7 times, assuming the lifetime of the chimney to be 30 years.

3.4 The mounting procedure

When manufacturing, the chimney is divided into a number of sections that are transported from the factory and welded together at the place of rising. At the chosen place, the armature is concreted to the ground, leaving the top of the bolts sticking up. Nuts are then mounted to the bolts, leaving them all horizontal. Four crosswise bolts are then turned a couple of turns. The chimney is thereafter raised, standing on those four crosswise bolts. Using nuts leaves the chimney standing vertically, even if the armature would have been concreted at an angle from horizontal. More nuts are then mounted to the bolts. The nuts of the four crosswise bolts, on which the chimney is standing, are tightened. All other nuts placed above the bottom guide ring are tightened with a torque, that pretensions the bolts. The nuts underneath the bottom guide ring are thereafter tightened.

Then 60 mm of thread of the bolts are taped, letting the pretension to be more stable against phenomena’s like creep. Finally, the armature is concreted, using expanding concrete, covering up to the bottom guide ring.

3.5 Further investigations

As mentioned in the Objective, the main thing is to analyze the lower parts of the chimney. An investigation of the geometry is needed and improvements are sought for. In order to find improvements the theory behind the dimensioning needed to be evaluated.

Due to the fact that there are various numbers of sizes of chimneys today manufactured, all with different loadings, the results of different analyses must be appropriately chosen. The idea of trying to find some kind of a so-called worst case scenario came up and was applied in order to eliminate the otherwise vast number of loading situations. This could be done by analyzing the input data given in Table 3-4, and the result is discussed in chapter 6. In the original objective, some kind of evaluation of the welding strength between the detailed parts of the chimney was considered. This is discussed further in chapter 5.

4 Problem description

As mentioned, the approach is to use a finite element solver to analyze the problem. But modelling all parts would not only be time demanding but it would also put a big effort on the computational strength. Before modelling could get started, some appropriate simplifications were needed to be done.

The purpose is, as mentioned, to in some way standardize the parameters of the lower parts of the chimney. Therefore all parts above these may be excluded. The existence of the excluded parts could, as a matter a fact, be replaced by an axial force, *F*, a shear force, *T*, and the moment, *M*, as given by the wind exposure analysis. In Figure 4-1 the replacements in terms of *F*, *T* and *M* are shown applies to the lower part of the chimney through application at one node at the centre of the lower cross-section.

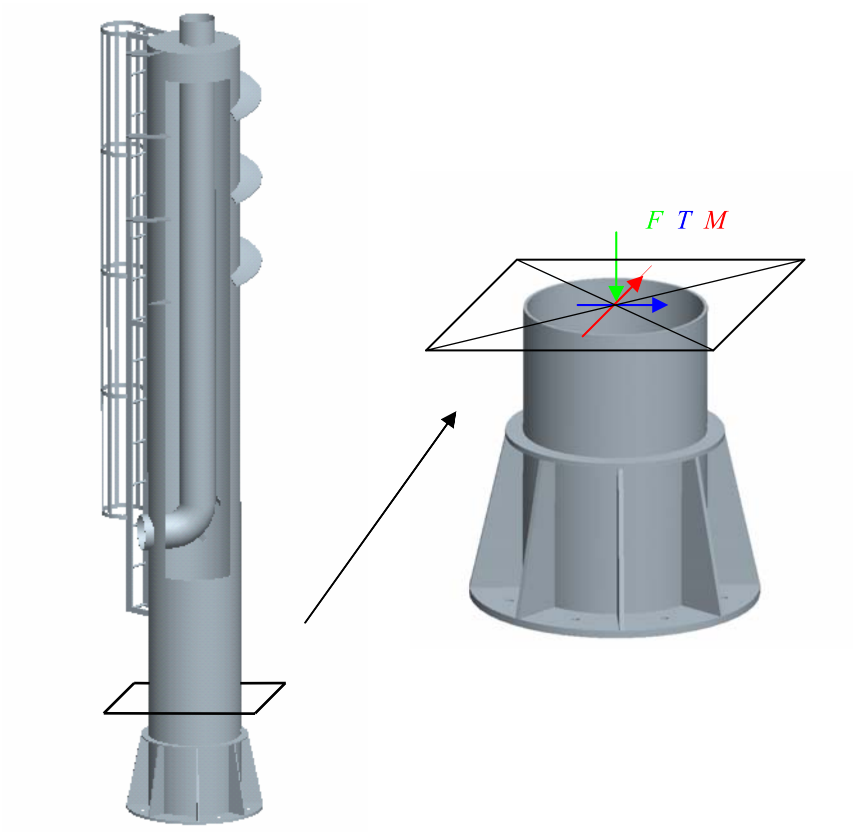

Figure 4-1. *Simplifications of the structure.*

Simplifications could also be made to the foundation on which the chimney is mounted. With the assumption that the concrete is rigid, it can be replaced by a rigid surface.

The bolts could, however, not be excluded due to the belief that the pretension they are exposed to would affect the results too much.

5 Theory

When dimensioning, not only static loading must be considered, but also phenomena's like fatigue and buckling must be evaluated. Even if the structure may look simple and smooth, the calculations are not trivial.

As mentioned the loading of the construction was determined according to the norms by the Snö och Vindlast (BSV97) in the wind exposure analysis. The strength of the structure was, however, determined using the norms of the Swedish norm BSK99. These norms are therefore also used in this Master's thesis, in order to make the results comparable.

In this chapter not only the theory of the BSK99 is presented, but also how it is applied to this problem.

5.1 *Yielding criterion*

5.1.1 Theory

The common dimensioning criterion when analyzing both static and dynamic loadings is that no yielding is allowed. One way of ensuring this is by applying the well known von Mises criterion which, for three dimensions using the six stress components $\sigma_x, \sigma_y, \sigma_z, \tau_{xy}, \tau_{xz}, \tau_{yz}$, is given by

$$\sqrt{\sigma_x^2 + \sigma_y^2 + \sigma_z^2 - \sigma_x\sigma_y - \sigma_x\sigma_z - \sigma_y\sigma_z + 3\tau_{xy}^2 + 3\tau_{xz}^2 + 3\tau_{yz}^2} \leq \sigma_{yield,Mises}$$

where $\sigma_{yield,Mises}$ is the yield strength of the material.

When dimensioning according to BSK99, safety factors are applied to take care of insecurities caused by geometrical deviations, uncertainties as concerns the loading situation, or other unknown stress intensity increasing circumstances.

For a plane stress state the criterion is given by

$$\sqrt{\sigma_x^2 + \sigma_y^2 - \sigma_x\sigma_y + 3\tau_{xy}^2} \leq \frac{f_{yk}}{\gamma_m\gamma_n} \qquad (5\text{-}1)$$

where f_{yk} denotes the yield strength in this formulation. The partial coefficient γ_m considers the tolerances when manufacturing and how this is affecting the ability of the component to withstand loads. The partial coefficient γ_n considers the consequences of what a failure may cause with respect to human and environmental damage. The values of the product of the partial coefficients with respect to the consequences of what a conceivable breakdown may cause are seen in Table 5-1.

Table 5-1. *Partial coefficient product,* $\gamma_m\gamma_n$.

Consequences of a breakdown	$\gamma_m\gamma_n$	Approximately failure risk
Neglected	1.0	10^{-2}
Less serious	1.1	10^{-3}
Serious	1.21	10^{-4}
Very serious	1.32	10^{-5}

5.1.2 Application

Fatigue is seen as the major cause for failure. If a breakdown would occur it could lead to catastrophic consequences, where both human and environmental health might be in great danger. Therefore the partial coefficient product here is put to

$$\gamma_m\gamma_n = 1.21 \tag{5-2}$$

using Table 5-1.

5.2 Fatigue criterion

5.2.1 Theory

When fatigue is considered, the stress width σ_{rd}, i.e. the difference between the maximum and minimum stresses at a point of the structure, is a very important variable. Also the number of applied cycles, n_t, is of great importance due to that the more cycles applied, the less the allowed stress width.

The dimensioning criterion according to BSK99 is given for normal stresses as

$$\sigma_{rd} \leq f_{rd} \tag{5-3}$$

and for shear stresses as

$$\tau_{rd} \leq f_{rvd} \tag{5-4}$$

where

$$f_{rd} = \frac{f_{rk}}{1.1\gamma_n}$$
$$f_{rvd} = 0.6 f_{rd} \tag{5-5}$$

It may be seen from the reduction of the allowed shear stress width that fatigue crack initiation is more vulnerable to shear stresses.

The characteristics of the strength fatigue parameter f_{rk} may be compared with the yield strength parameter f_{yk}, but depends on the number of cycles, n_t, and the manufacturing parameter, C, according to Figure 5-1 . The manufacturing parameter C considers geometrical variables such as the roughness of the surface. It may be seen that if the manufacturing restrictions are high it leads to higher allowed stress width. It may also be seen that when the number of cycles is very large, some kind of fatigue threshold appears.

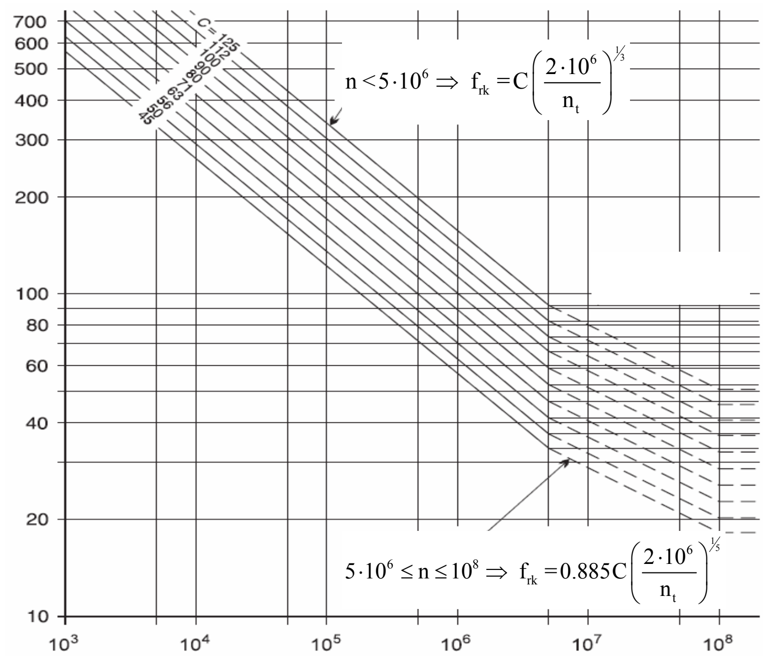

Figure 5-1. *Allowed stress width f_{rk} with respect to manufacturing parameter C and number of cycles n_t.*

Due to the variation in stress width between the loading cases, i.e. wind gusts and vortex shedding, the Palmgren-Miner's fatigue hypothesis is used:

$$\sum\left(\frac{n_t}{n_{ti}}\right)\leq 1.0 \qquad (5\text{-}6)$$

where n_t is the number of cycles applied and n_{ti} is the number of cycles to failure of the structure.

5.2.2 Application

As a notice, it may be seen in equations in Figure 5-1 that the vortex shedding is more harmful than the wind gust when loading with an equal stress width due to the larger number of cycles. This is the reason for applying chimney spirals to decrease the stress width for these harmful vortex sheddings. Applying too many chimney spirals leads, however, to heavily increased loading due to the wind gust and, therefore, a balance of chimney spirals lengths must be found. This is investigated in the wind exposure analysis.

For CorTen, which is a rolled sheet manufactured according to performance class GB, the *C* parameter is given as

$$C = 112 \text{ MPa}$$

A conservative way of achieving the stress width is by the use of the principal stresses instead of the six stress components $\sigma_x, \sigma_y, \sigma_z, \tau_{xy}, \tau_{xz}, \tau_{yz}$ that usually are obtained from the FE-analysis. The principal stresses $\sigma_1, \sigma_2, \sigma_3$ are trivially calculated from the Mohr's circle when knowing the stress components. Figure 5-2 is showing the Mohr's circle for stresses, but the formulas of how to obtain the principal stresses are here omitted.

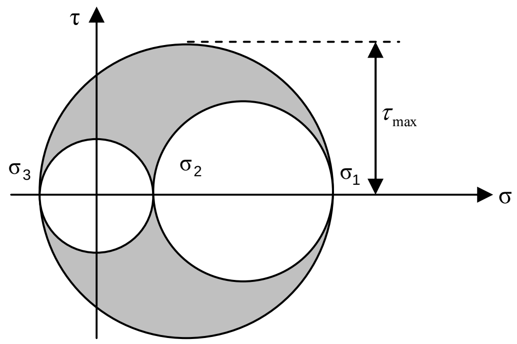

Figure 5-2. *Mohrs circle of stresses with the principal stresses* $\sigma_1, \sigma_2, \sigma_3$ **.**

Due to the fully generically symmetric fatigue loading, the maximum stress width may be determined as the difference between the maximum principal stress on the, so-called, tensioned side and the minimum principal stress on the, so-called, compressed side, see Figure 5-3. Due to the fatigue loading, the tension and compression stresses change with the deformation of the chimney.

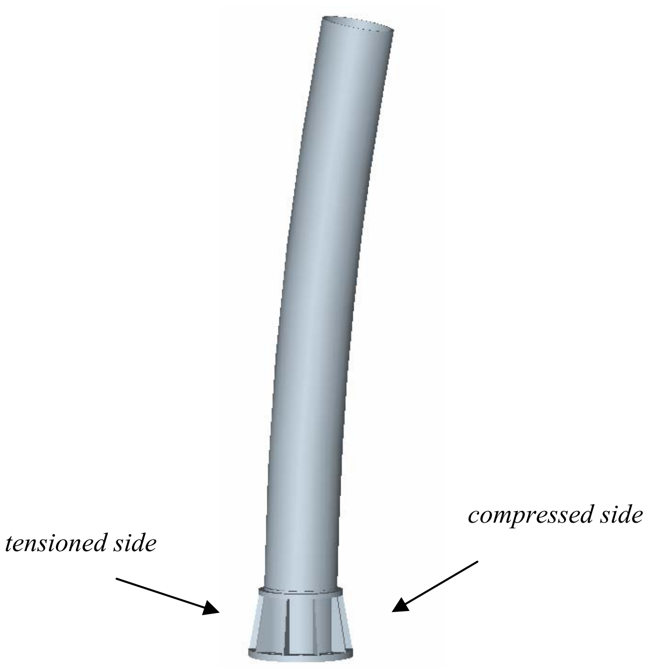

Figure 5-3. *The tensioned and compressed side of the chimney.*

The advantages of using the principal stresses is that, instead of evaluating all stress components, only one evaluation is needed, namely

$$\sigma_{\mathrm{rd}} = \left(\sigma_1 - \sigma_3\right)$$

where σ_1 is the maximum principal stress on the tensioned side and σ_3 is the minimum principal stress on the compressed side.

The harmful shear force is actually not an issue due to that it is included in the previously given equation. As seen in the Mohr circle, the maximum shear stress $\tau_{\max}$ is given by

$$\tau_{\max} = \frac{(\sigma_1 - \sigma_3)}{2}$$

The shear stress changes direction when the loading is fully cyclic, like in this case of the chimney. However, the ratio between the maximum difference between the principal stresses and the difference between the maximum shear stresses is equal to 0.5. This is clearly seen in Mohrs circle of stresses, see Figure 5-4. When evaluating the shear stress, however, a factor 0.6 was used, cf. equation (5-5). Thus the dimensioning is conservative.

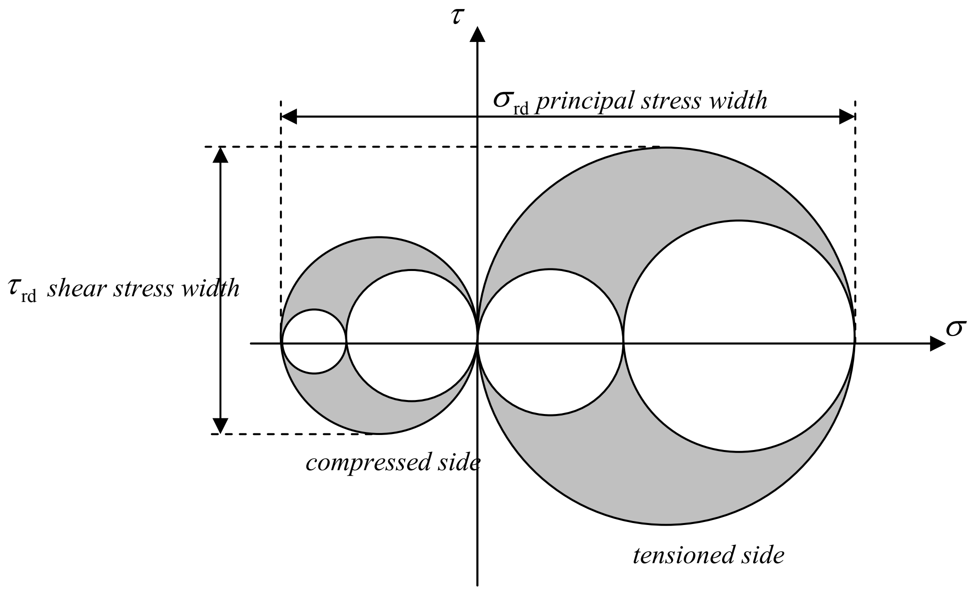

Figure 5-4. *The difference between the principal stress width and the shear stress width.*

5.3 Corrosion

5.3.1 Theory

Corrosion is a problematic subject but, when the assumed lifetime is known, the surroundings are well known, the material behaviour is well known and the risk for extreme corrosion phenomena's as point corrosion is low, an addition to the thickness of the sheet may be added to compensate the effects of corrosion. This addition may be seen in Table 5-2, where data are given for pure steel and corrosion resistant steel of different corrosion classes.

Table 5-2. *One sided corrosion of sheet made of steel.*

Corrosion class	First 10-years period		Following 10-years period	
	Steel	Corrosion resistant steel	Steel	Corrosion resistant steel
C2	0.05 mm	0.02 mm	0.015 mm	0.01 mm
C3	0.12 mm	0.08 mm	0.06 mm	0.05 mm

C4	0.30 mm	0.15 mm	0.20 mm	0.10 mm

5.3.2 Application

As mentioned the chimneys are constructed from sheet metals made of CorTen. This steel is a corrosion resistant material and categorized as corrosion class C4. The chimneys lifetime is, as mentioned, put to 30 years. From this information, the addition needed easily is determined to 0.35 mm.

When manufacturing sheet metal there are different standardized thicknesses available. Therefore the addition needed to compensate for the effects of corrosion is included, and in the calculations and modelling excluded. This means, for example, that when choosing the thickness 12 mm when manufacturing the sheet metal supports, only 11.3 mm may be used when modelling.

Further, it is believed that no corrosion appears inside of the casing due to the advantageous environmental conditions caused by the heat from the flue pipes. In addition, no corrosion is expected on the concreted side of the bottom guide ring.

5.4 Buckling criterion

5.4.1 Theory

Buckling is a very complicated collapse mode and experience is necessary to handle these kinds of problems. Buckling only occurs when pressure is applied to the structure.

Analyzing buckling with FEM is very problematic, due to that imperfections are difficult to include in the model. To that end some kind of disturbance has to be applied, either as geometrical imperfections or by applying forces imperfect. The magnitude of the imperfection also affects the result and must therefore be carefully chosen. Buckling occurs when the loading of the structure exceeds the bifurcation point of the structure.

In Figure 5-5, a beam is loaded with an axial force *P* which is compressing the beam. A disturbing force *F* is applied at the centre of the beam. If no disturbing force is applied the beam may be loaded with a very high load *P*, and no buckling will occur. But if applying a disturbing force *F*, buckling occurs in terms of large deflections of the beam from the centre line. The deflection is depending on the size of the disturbing force. The same phenomenon would appear if the shape of the beam would be disturbed.

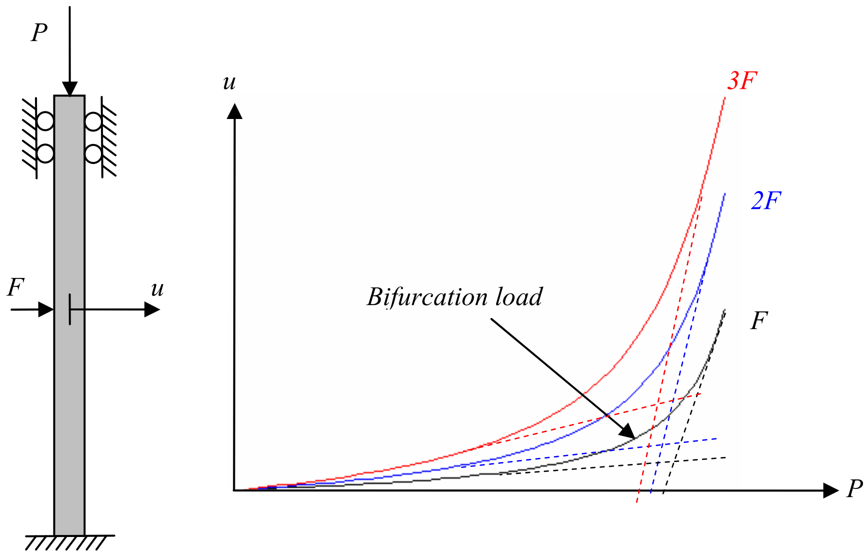

***Figure 5-5.** The loaded structure with the bifurcation investigated with respect of disturbing force.*

5.4.2 Application

When manufacturing, restrictions are often posed on geometrical uncertainness. For the sheet metal support these restrictions are, approximately, given by the deflection of an I-beam according to the BSK99 standard, see Figure 5-6.

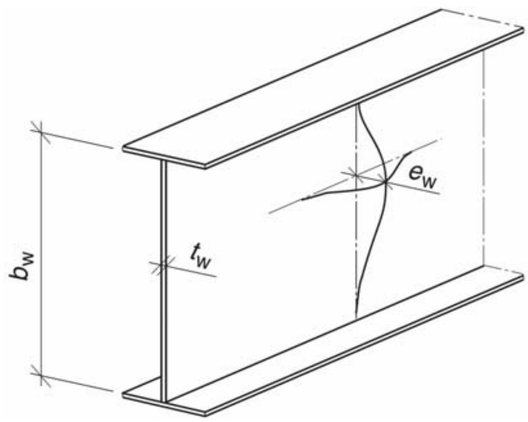

$$e_w \leq \frac{b_w}{200} \quad \text{if} \quad \frac{b_w}{t_w} \text{ £ } 80$$

$$e_w \leq \frac{b_w^2}{16000\, t_w} \quad \text{if} \quad 80 < \frac{b_w}{t_w} < 200$$

$$e_w \leq \frac{b_w}{80} \quad \text{if} \quad \frac{b_w}{t_w} \leq 200$$

Figure 5-6. *I-beam with restrictions on deflection.*

Due to the slenderness and by knowing the height b_w and the thickness t_w of the sheet metal supports, the maximum deflection e_w may be calculated according to

$$\frac{b_w}{t_w} = \frac{0.5}{0.012} \leq 42 \leq 80 \quad \Rightarrow \quad e_w \leq \frac{b_w}{200} = \frac{0.5}{200} = 0.0025\,\text{m} \qquad (5\text{-}7)$$

5.5 Pretension

The bottom guide is, as mentioned, mounted to a bolt armature and works like a screw joint. For a screw joint to work properly and resist large amounts of static and fluctuating loads during long periods of time, the screws have to be pretensioned. The pretension should be kept at certain level so that the compounded stress (tensioned and twist stresses) in the screws do not exceeds the yield strength of the screw material. The pretension load main function is to pinch together the unite parts. This also prevails the screw and the nut to loosen and accomplish frictional forces between the pinched parts, which counteract shear forces. A joint with high pretension becomes less vulnerable to fatigue than a joint with lower pretension. The pretension that applies during mounting can gradually decrease through composition (settling) of the pinched material, i.e. a part of the plastic deformation will be permanent. To not decrease the pretension too much, the screw joint should have a certain pinch length. The elastic elongation of the screw could then countervail some of the composition.

To get a specific pretension force in the joint, a tightening moment is applied with a wrench key according to calculations. One way of checking that the pretension gets large enough to keep the joint together and also checking that the load on the screws does not get too high when an external force is applied, is to use a force-strain-diagram, where forces illustrates both the screw and the ground material. See figure 5-7 for an example of a diagram with a screw joint applied to an external force and with pretension.

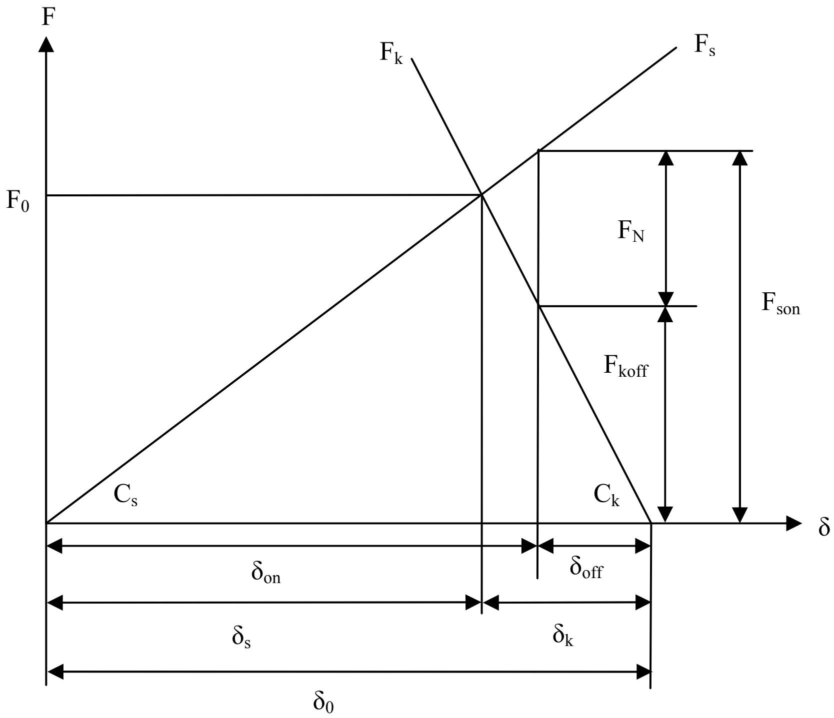

δ_{on} = deformation of the parts that are loaded; δ_{off} = deformation of the parts that are unloaded

δ_s = strain of the screw; δ_k = compression of the ground material; C_s, C_k = rake of the lines $= \dfrac{E \cdot A}{L}$

Figure 5-7. *Force-strain-diagram of a screw joint.*

The diagram shown in Figure 5-7 illustrates how the external force F_N will influence the joint. The current screw force, F_s increases and the strain δ_s increases in the screw due to the external force. The current contact force on the ground material F_k decreases, which implies less pressure towards the ground material. The current force of loading parts F_{son} cannot exceed the yielding stress of the screw, and the current force of unloading parts F_{koff} cannot get too small compared to the external force F_N, because then the joint will separate.

An optimal way of using the screw joint is to pretension the screws as much as to reach into the yielding point and get minor dispersion of the pretension force. According to BSK99 considering pretensioned bolts, only 20 % of the stress width in the fatigue analysis should be encounted for. According to the analytical calculations made by Gullmanders Arking AB the pretension force of the M24 bolts (except the four crosswise bolts) is set to 76400 N and the elongation δ_s will then be 0.124 mm. The four crosswise bolts are just tightened so that they carry the weight of the chimney.

5.6 Welding evaluation

The different parts of the chimney are mounted together by welds of certain kinds, depending on which critical area the wind load are hitting at during exposure. In figure 5-8 it is shown how the parts are attached to the lower part of the chimney.

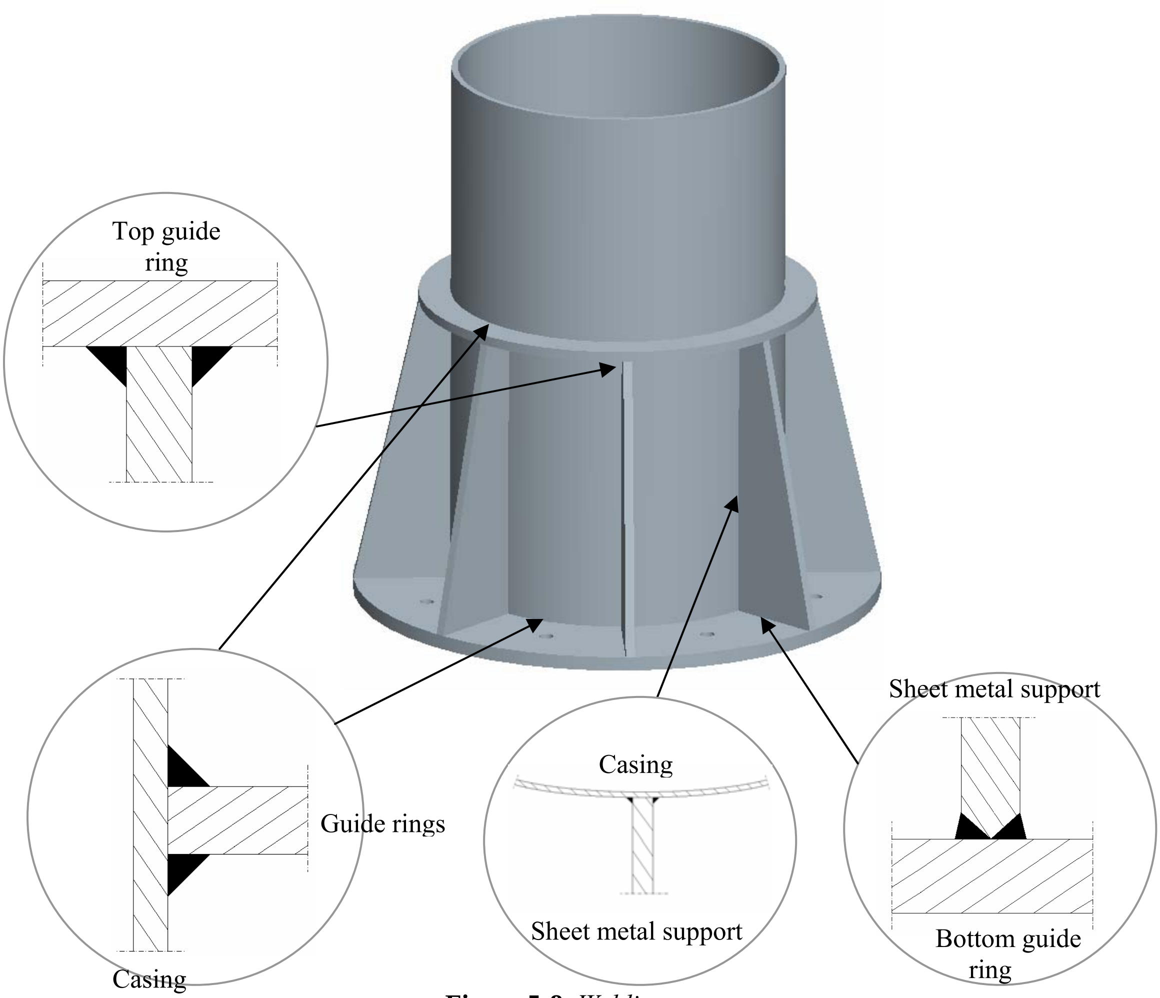

Figure 5-8. *Welding map.*

As mentioned in previous chapters some kind of welding evaluation was considered. These welds were not modelled in the analysis due to use of shell elements. In the welding analysis it showed that probably no improvement was able to be done due to the lack of methods used, i.e. poor mesh size and no welds were therefore modelled.

6 Approximations

In order to reduce the number of parameters, the input data were evaluated, searching for a parameter combination constituting a worst-case scenario.

6.1 Axial force

The axial force represents the weight of the casing and the parts connected to it, such as the ladder and the flue pipes. It is not surprising that the weight depends on the dimension of the chimney. Therefore a worst-case approximation is sought for.

The weight W of the casing is given by

$$W = \rho V g \tag{6-1}$$

where ρ is the density of the material, V is the volume and g is the acceleration due to gravity. If assuming the casing to be thin walled, with the diameter D, and with no change in thickness t through the sections, and chosen from the ground section of the casing and assumed constant through the height h, the volume V is given by

$$V = hD\pi t \tag{6-2}$$

The height h of the chimney is restricted by the aspect ratio and given as

$$h \leq 40D \tag{6-3}$$

Equations (6.2) and (6.3) inserted into (6.1) leads to the maximum weight of the casing according to

$$W = \rho(40D^2\pi\, t)g \tag{6-4}$$

The weight of the ladder and the flue pipes is assumed to never exceed the weight of the casing itself, giving the final axial force F_{axial}

$$F_{axial} = 2W = 2\rho(40D^2\pi\, t)g \tag{6-5}$$

In Figure 6-1 the axial forces from the data given in Table 3-4 are shown under the above assumptions. Due to the approximations it might be noticed that the chimneys with higher aspect ratios are well represented by the approximations, while the approximations give poor results for chimneys with lower aspect ratios.

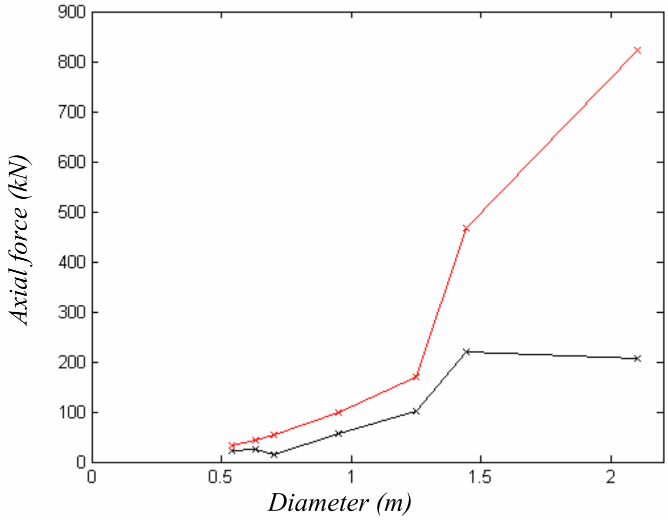

Figure 6-1. *The approximated axial force (red) compared to the actual axial force (black).*

6.2 Shear force

Finding a relation between the shear force and the moment is not trivial. The aspect ratio is, also here, vital. With a high aspect ratio, the ratio between the moment and shear force is high. The presence of chimney spirals also affects the result. Figure 5-1 shows the aspect ratio between the moment and the shear force for the casings given in Table 3-4. All three loading situations are considered.

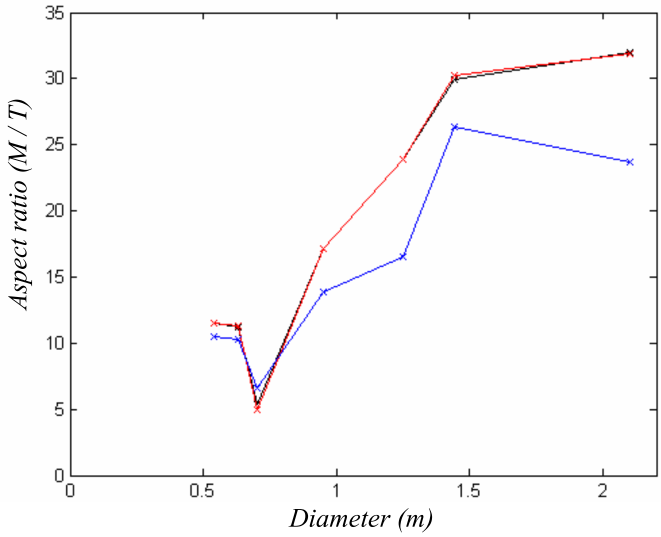

Figure 6-2. *Ratio between the moment and shear force;*
Static load (black), Wind gust (red), Vortex Shedding (blue).

It might be seen that the ratio only once is below 10, and this is for the chimney with diameter 0.7 m. However, relatively low forces and moments are obtained due to that the aspect ratio for this chimney is low. A conservative estimate is, therefore, to adopt the ratio between the shear force T and the moment M according to

$$T = \frac{M}{10}$$

Another issue is whether the shear force affects the system or not, due to the small distance between the force and the parts it is supposed to affect.

7 Modelling

7.1 Numerical formulation

In this project the commercial finite element code ABAQUS is used.

7.1.1 Parameterisation

Due to the large number of possibilities of constructions subjected to a number of different loadings, some kind of parameterisation seems necessary. Using ABAQUS this was only possible by writing a script in the Python language. Parameterisation gives a great number of advantages; not only the size of different parts but also the number of sheet metal supports and bolts, could be arbitrary chosen. Also, modelling parameters like mesh size could be defined between different parts by letting common edges have equal number of nodes for every geometry combination used.

Due to the slender detailed parts in the structure, a shell-based model could be created without losing too much accuracy in the calculations. When using shell elements, the geometry of the structure has to be modified due to that the thickness is defined at the centre of a part. The modifications may be seen in Figure 7-1.

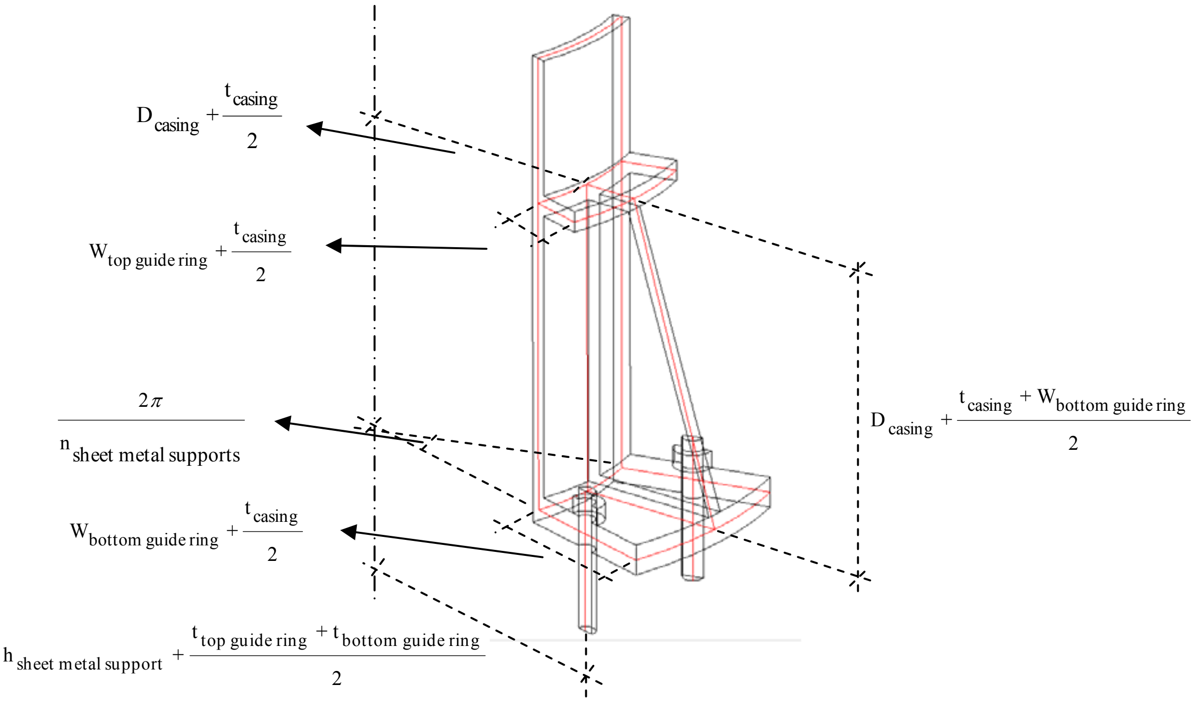

Figure 7-1. *The modified geometry.*

Due to symmetry only one parameterised section, consisting of a slice of the casing and the top and bottom guide rings, one bolt element and one sheet metal support, was modelled. This section was then patterned into the desired model containing all of the sheet metal supports; bolts, guide rings and casing. The foundation was modelled as a rigid plate, see Figure 7-2.

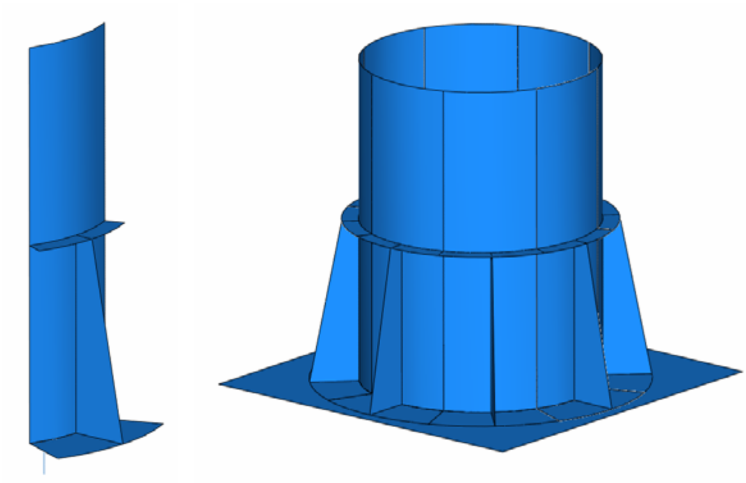

Figure 7-2. *Parameterized section (left) patterned into the total structure (right).*

7.1.2 Element type

Shell elements were used when modelling all parts, except the bolts. The element type chosen was the group of conventional shell elements for which only, apart from geometry and material properties, the thickness of the shell was needed to be given. Due to the simple geometry, quadratic elements could be used, and avoidance of the stiffness increasing triangular elements obtained. Because of the intuitively assumed presence of bending moments in the structure, reduced integrations was chosen. Due to the contact between the bottom guide ring and the rigid body, first order, linear, elements were used, not only here but also in the full model.

The bolts were modelled as wires, prescribed as beam elements. They were given parameters like material data, circular cross section and also beam section orientation, which, however, in our case was, unimportant due to the symmetrical cross section.

7.1.3 Mesh

When creating the mesh, it is made continuous between the parts. This gives benefits in the interactions. The shapes of the elements are chosen so that they remain as quadratic as possible, i.e. the aspect ratio is kept close to one and the distortion of the shape of the elements is as small as possible. The sizes of the elements are, for the buckling analysis, chosen so that the differences between the nodal stresses are minimized as compared to the elemental stresses, without making the mesh too dense. For the strength analysis and the welding evaluation the mesh is sized so that, at least, one element fit in the intended weld.

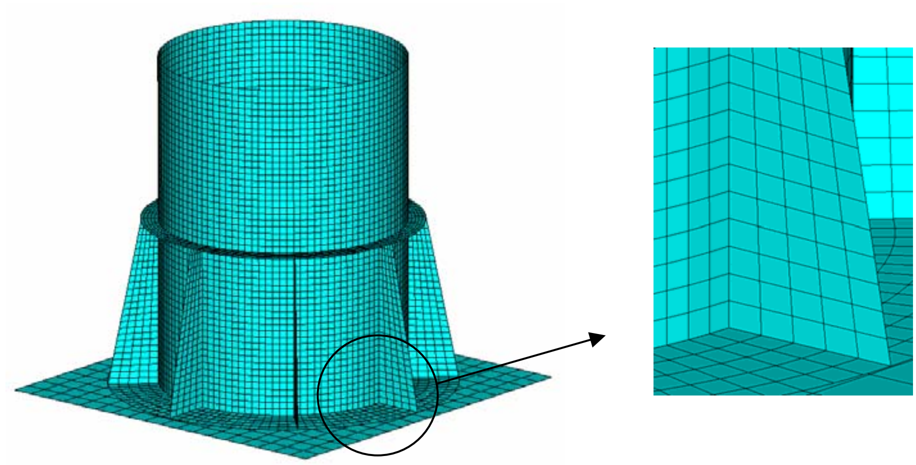

Figure 7-3. *The mesh.*

7.1.4 Materials

A material behaviour was prescribed for each part. The sheet metal supports, the casing and the guide rings were CorTen, while the bolts were steel SS2134.

Due to that no plasticity was expected in the structure, together with the assumption that CorTen and SS2134 are isotropic, very simplified linear elastic material models were created with only the densities, Young's modulus and Poison's ratios given as material parameters.

7.1.5 Constraints

To connect different parts to each other, constrains were used in form of ties. By setting tie constrains, the bodies are modelled as glued together. By having the same refinement of the meshes in the constrained areas, which, in our model, were obtained by parameterization, the nodes on each part will be common. This leads to that the stresses will be continuous between the tied parts. In this model node-to-surface constraint enforcements are used, where the rotations between constrained surfaces are prohibited. The bolts are also restricted by the tie constraint, due to the mounting against the bottom guide ring.

To apply the loading a one-node body is placed at the top centre of the modelled casing. This body is then coupled to the top of the casing so that the loading, in terms of a shear force, an axial force and a moment, is applied to the structure, see Figure 7-4.

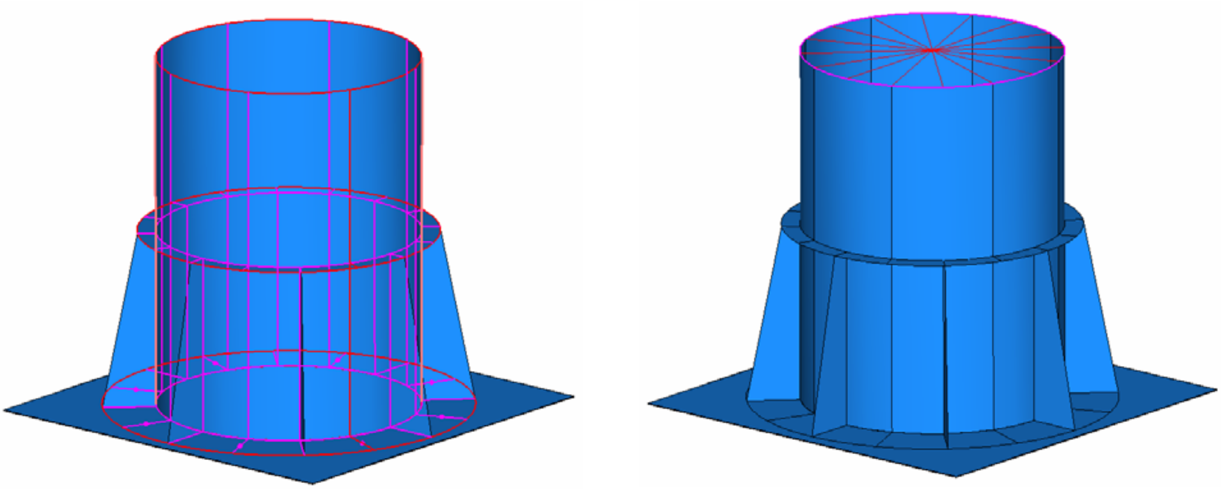

Figure 7-4. *Constraints: Tie between different parts (left) and coupling to a single node (right).*

7.1.6 Boundary Conditions

The bolts are locked in all degrees of freedom at their lower nodes, which models the reality well due to that the concreted armature may be considered rigid. Due to that the bolts are able to be extended, the upper nodes are locked in all degrees of freedom except from the vertical direction. The constraint between the lower guide ring and the bolts will lead to that no horizontal rigid body motion appears.

The rigid surface that represents the foundation at which the chimney rests is also, naturally, locked in all degrees of freedom, see Figure 7-5.

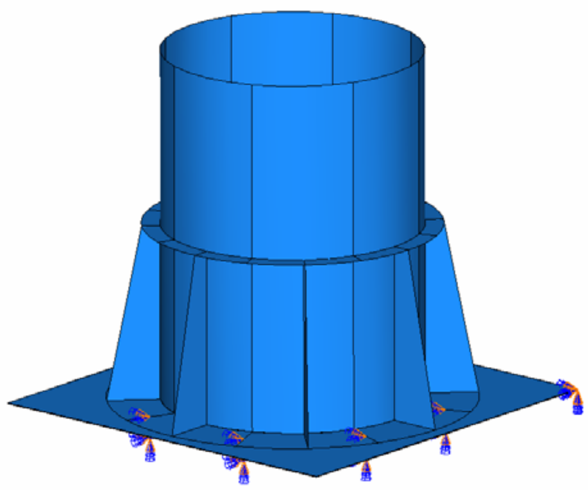

Figure 7-5. *Boundary conditions.*

7.1.7 Interactions

The only interaction between parts that appears in the model is the contact between the lower guide ring and the rigid surface. Due to that the bolts are preventing the chimney from sliding on top of the foundation, no tangential contact behaviour was needed to be modelled. The only contact property set was the normal contact behaviour, which was given as “hard”. The interaction leads to that penetration through the rigid plate is prevented, see Figure 7-6.

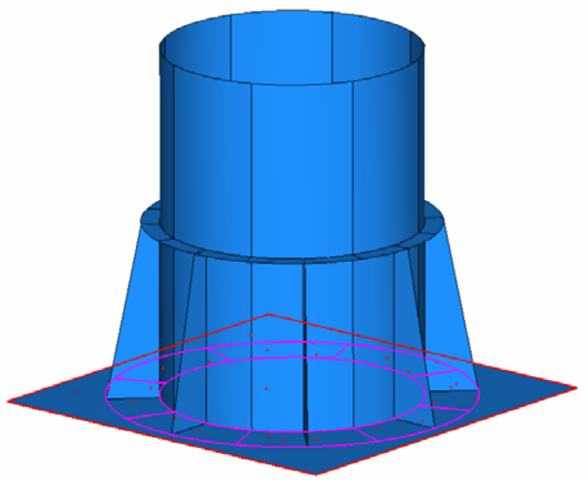

Figure 7-6. *Contact between bottom guide ring and rigid body.*

7.2 Loading

When the model is created and all constrains, such as the interactions and boundary conditions, are applied, the loadings may be set. This was done in four steps in order to model the actual loading situation as accurate as possible.

7.2.1 Step 1: Gravity and weight

Due to that only the base of the chimney is modelled, a vertical force that represents the weight of the structure is applied to the coupled node. The coupling will divide the force onto the casing in a natural manner. The modelled parts are given gravity, which, in the combination with the previously given geometry and density, gives the weight of the modelled parts, see Figure 7-7.

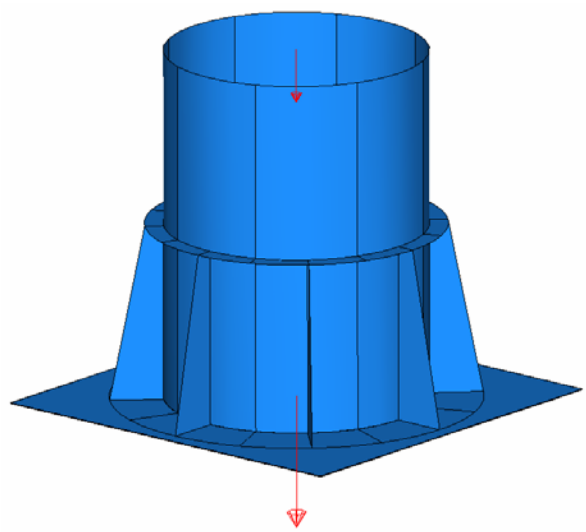

Figure 7-7. *Gravity and weight applied on the structure.*

7.2.2 Step 2: Mounting procedure

By setting a boundary condition where the lower nodes of the bolts are moved downwards, a pretension effect occurs. The distance of movement is the earlier calculated distance due to pretensioning. This is only applied to the bolts that are pretensioned. The lower nodes of the four crosswise bolts are moved upwards, so that they carry the total weight of the structure given in equation (6.5), corresponding to the mounting procedure, see Figure 7-8.

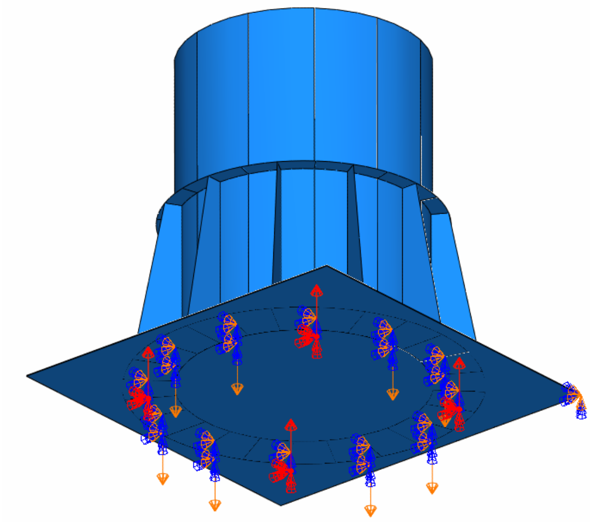

Figure 7-8. *Mounting procedure; four crosswise bolts (red) and pretensioning (brown).*

7.2.3 Step 3: Disturbing forces

Due to the lack of imperfections in the model itself, disturbing forces are applied to the sheet metal supports on the buckling side of the structure. These forces are experimentally determined so that the theoretical deflection given by equation (5.7) is obtained. The disturbing forces are only applied when buckling is to be analyzed, and not when the strength of the structure is investigated because of the additional stresses they cause, see Figure 7-9.

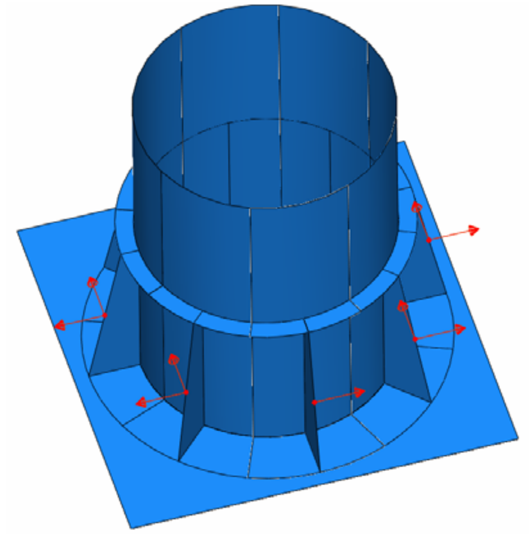

Figure 7-9. *Disturbing forces acting on the sheet metal supports.*

7.2.4 Step 4: Applying loading

The loadings in terms of a moment and a shear force are, as earlier described, applied to the constrained one node body at the top centre of the casing, see Figure 7-10. During the buckling analysis the loading was linearly ramped up in a number of steps until the bifurcation point of the structure was reached.

When analyzing the strength of the different parts, the loading was increased until yielding appeared.

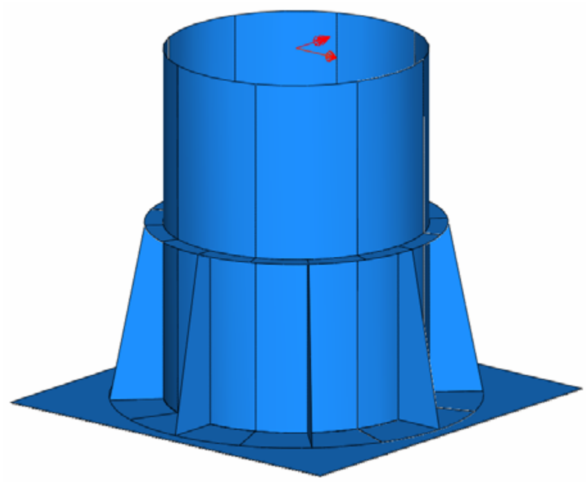

Figure 7-10. *Load appliance; shear force and moment.*

8 Verifications

In order to assure that the model is acting as expected, some verifying calculation were performed. Due to the simple loading situation the intended response of the structure could easily be compared with the results from the FE-analysis. The parameters used for verification are shown in Table 8-1.

Table 8-1. *Parameters used for verifications.*

Parameter	Value
Casing diameter	500 mm
Casing thickness	6 mm
Axial force	29 kN
Disturbing force	8 kN
Momentum load	150 kN
Number of sheet metal supports	12
Sheet metal support thickness	8 mm

8.1 Step 1: Gravity and weight

The response from applying the gravity together with axial forces, i.e. the weight, may be seen in Figure 8-1.

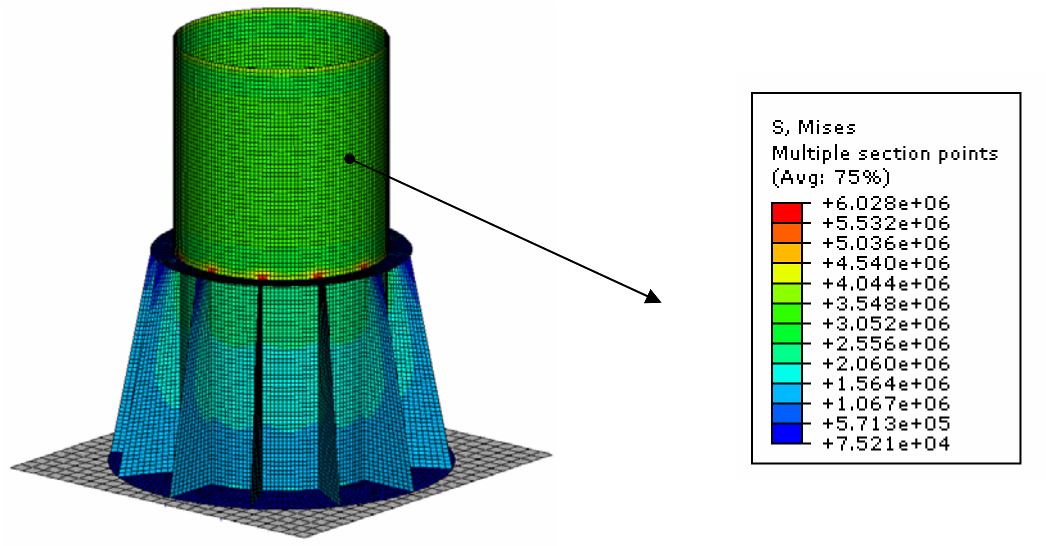

Figure 8-1. *Response from applying gravity and axial force.*

The response is, as assumed, symmetric, and the stresses are not surprisingly low. The bottom guide ring is in contact with the rigid plate, as expected. The axial stress σ_{axial} in the casing may easily be calculated by using the definition of stress according to

$$\sigma = \frac{F}{A}$$

where *F* is the force acting on the projected area *A*.

If approximating the casing as thin walled with circular cross section of thickness *t* and diameter *D,* the axial stress σ_{axial} may be approximated by

$$\sigma_{\text{axial}} = \frac{F_{\text{axial}}}{\pi D\,t} = \frac{290000}{\pi 0.5(0.006 - 0.00035)} \approx 3.3 \ \text{Mpa}$$

It is seen that the calculated stress is equal to the stress obtained from the FE-analysis, which verifies the correctness of choice of application of axial force and gravity.

Also notable is that the highest stresses appears at points where the casing, top guide ring and sheet metal supports are welded. This is not surprising due to the increased stiffness of the structure at these points. The absolute value of the stresses at these points may, however, not be true due to singularity phenomena because of the geometrically transitions. It is also seen that the stresses are decreasing down the structure due to the increasing cross section area.

8.2 Step 2: The Mounting procedure

The pretension of the bolts is the most difficult part to simulate. During the mounting procedure the chimney is standing on the four cross wise bolts before the foundation is finally concreted. This gives the bottom guide ring a deformed shape, which not was modelled in the FE-simulation due to the approximation of using a rigid surface, making the bottom guide ring flat. How much this affects the system is unknown and must be evaluated separately. The mounting procedure was thus performed by moving nodes, and, intuitively, this feels like a reasonable approximation. The result from the FE-analysis may be seen in Figure 8-2.

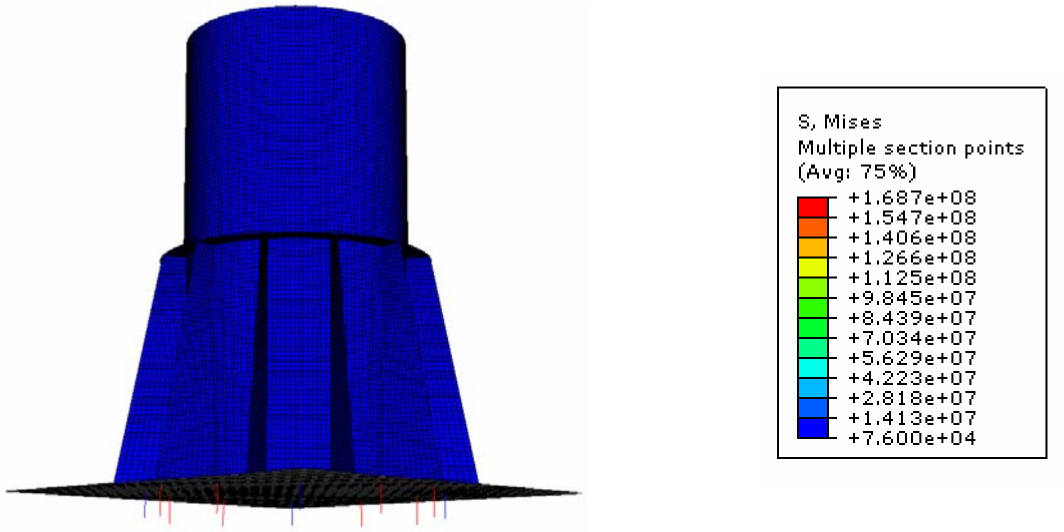

Figure 8-2. *The response from the mounting procedure.*

The result shows that the pretensioned bolts hold a stress of approximately 170 MPa, which is approximately the stresses it was supposed to gain.

The four crosswise bolts, with nodes moved upwards, were subjected to compressive stresses of -18 MPa. The stresses were somewhat lower than expected, but this was because the lower guide ring got deformed so that the upper node could move upwards. The influence from these four bolts on the bottom guide ring may be seen in Figure 8-3.

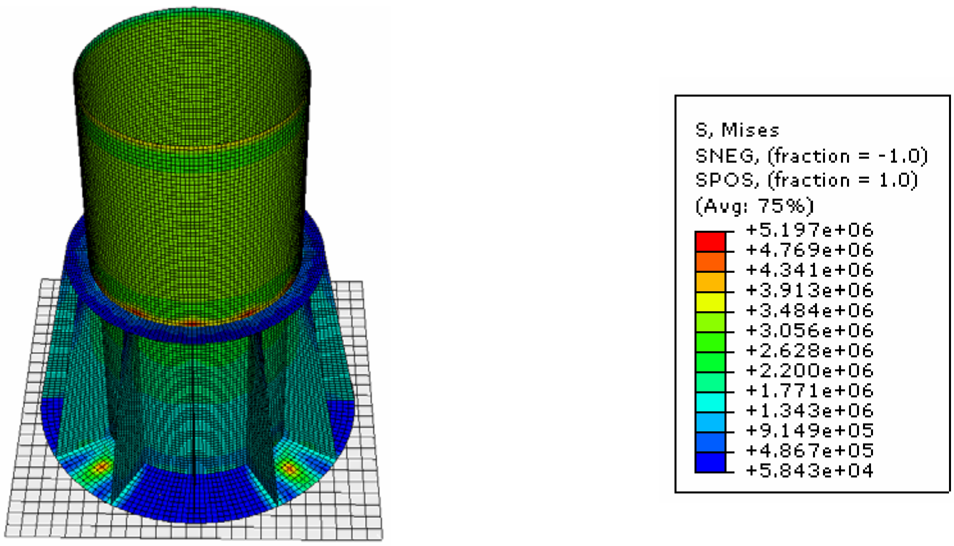

Figure 8-3. *The influence from the four crosswise bolts may clearly be seen in the bottom guide ring.*

8.2.1 Step 3: Disturbing force

The direction of disturbing force application is easy to verify by investigating the deformation. As seen in Figure 8-4, the sheet metal supports are deflecting in the same direction as the disturbing force was applied. The deflections of the sheet metal supports are continuous and are, as expected, largest at the points of the disturbing force application. The deflection is measured to approximately 2.5 mm, which was the restriction put according to the norm BSK99.

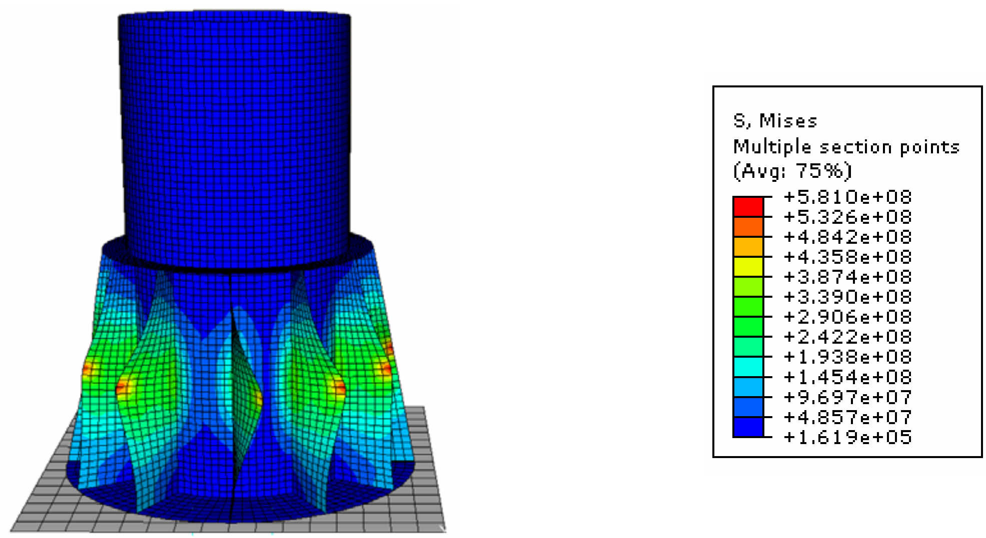

Figure 8-4. *The response of the disturbing forces.*

It may be seen that singularities appear at points where the disturbing force was applied, but a couple of nodes away from these areas the stresses are, approximately, 300 MPa. Due to the large effects the disturbing force has on the structure, only the effects at dimensioning from this force on buckling will be considered, and no induced stress values may be used for further analysis.

8.2.2 Step 4: Applying loading

It is expected that the casing will bend in the direction of the shear force at load application. Intuitively the sheet metal supports on this side are expected to be compressed, whereas the sheet metal supports on the other side should be exposed to a tension. On the compressed side of the chimney the bottom guide ring rests on the rigid plate while it, on the other side, wants to leave, and is at this stage only connected to the bolts, which gets extended, see Figure 8-5.

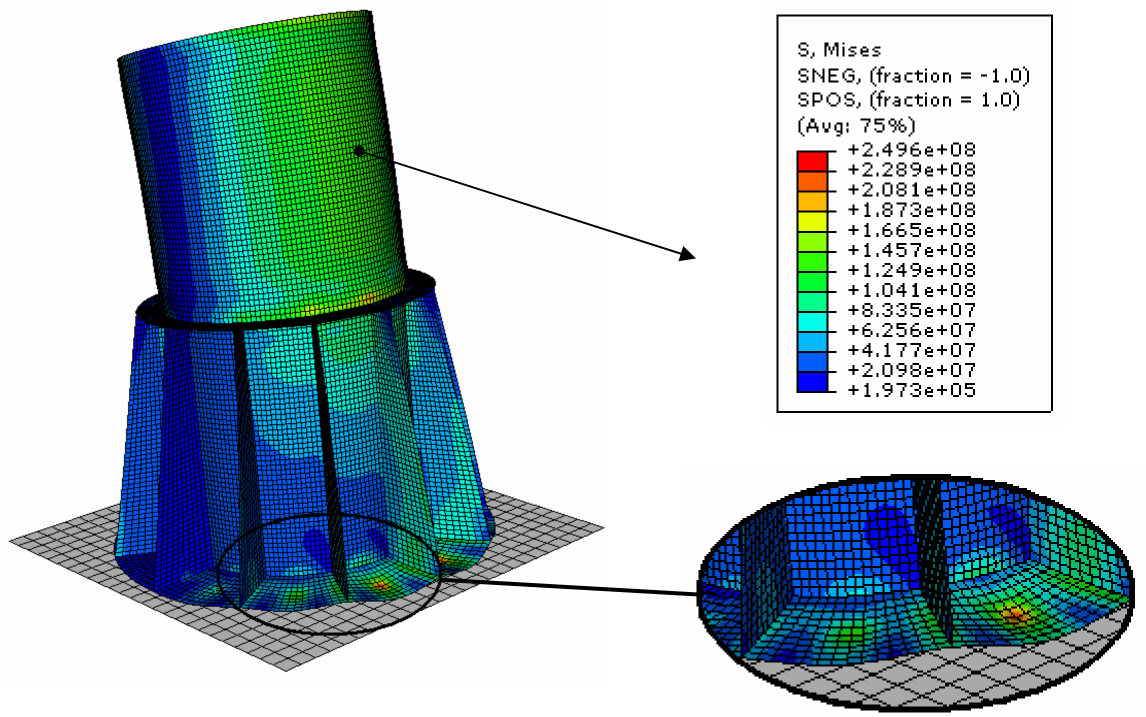

Figure 8-5. *The response of the chimney when loaded.*

The maximum axial stress $\sigma_{\text{axial,max}}$ in the casing may approximately be calculated using the Euler-Bernoulli beam theory according to

$$\sigma_{\text{axial,max}} = \frac{F}{A} + \frac{M}{W_b}$$

where F is the axial force, M is the applied moment, A is the cross section area and W_b is the section modulus.

If approximating the casing to be thin walled, having a circular cross section with thickness t and diameter D, the stress σ_{axial} may be estimated to

$$\sigma_{\text{axial}} = \frac{F_{\text{axial}}}{\pi D t} + \frac{M_{\text{load}}}{\pi (D/2)^2 t} =$$

$$= \frac{290000}{\pi 0.5(0.006 - 0.00035)} + \frac{150000}{\pi\, 0.25^2 (0.006 - 0.00035)} \approx 138\,\text{Mpa}$$

It might be seen that the calculated stress is, approximately, equal to the stress obtained from the FE-analysis, which verifies the application of the loading. The effect of the shear force is neglected in the analytical calculation, but even so the axial stress in the casing is close to the calculated, which indicates that the previous discussion concerning the minor effects of the shear force is valid.

8.2.3 Force equilibrium

The model seems to respond as predicted, but finally are the reaction forces investigated to make sure that all quantities are within their ranges. In this Master's thesis, only the vertical equilibrium for Step 2 is presented due to the simplicity in evaluating the result, but equilibrium, of course, holds for all directions and steps. The moment equilibrium is, likewise, satisfied. See figure 8-6.

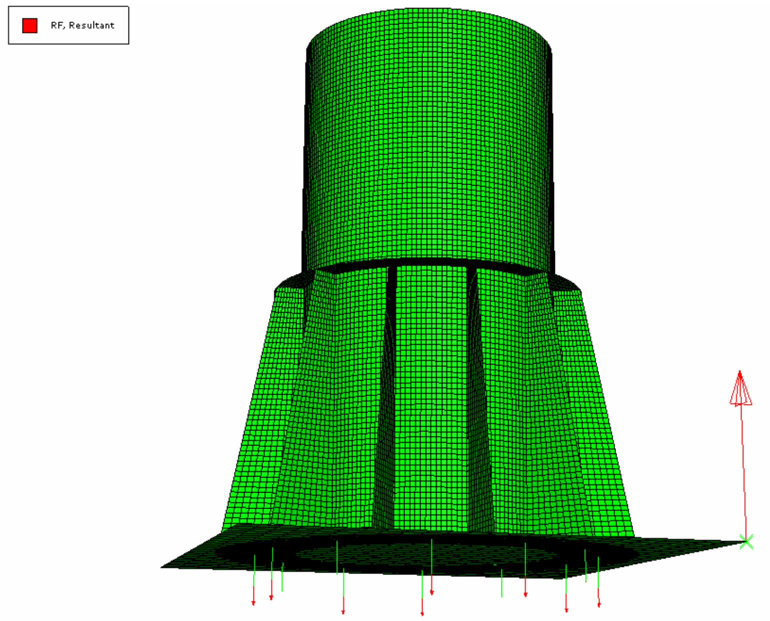

Figure 8-6. *Force equilibrium for step 2, applied weight and preloading.*

9 Buckling analysis

9.1 Analytical calculations

The current calculations against buckling are extremely simplified. The weld between the casing and the sheet metal support is neglected, which leads to that the Euler buckling formulas may be used.

The approximation intuitively leads to that the stiffness significantly decreases due to that the weld between the casing and the sheet metal support is neglected. This gives a conservative result, leading to increased thickness of the sheet metal supports.

9.2 Numerical simulation

The disturbing force was experimentally chosen so that the deflection was fulfilling the requirements of BSK99 given in equation (5.7).

A couple of calculations with various thicknesses of the sheet metal supports were performed. The loading, in terms of moment and shear force, was ramped linearly until buckling could be investigated by visualization of the so-called bifurcation. The displacement was measured on the sheet metal support at the point of maximum deflection, which coincided with the node where the disturbing force was applied, see Figure 9-1.

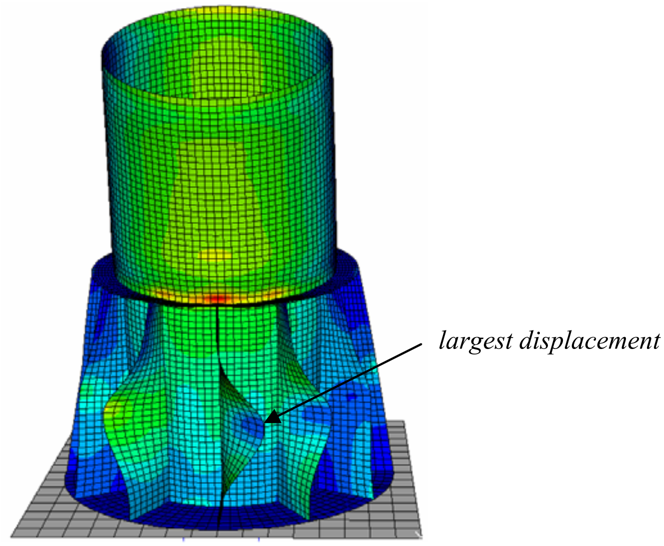

Figure 9-1. *The point where the displacement of the sheet metal support is measured.*

9.3 Results

It could clearly be seen that buckling was not an issue. Either yielding or buckling at other places of the structure appeared long before the bifurcation became visible in the sheet metal support. Therefore the thickness of the sheet metal supports was decreased to 8 mm, which became the new standard. A thinner sheet metal support could be chosen with respect to buckling, but the chosen thickness must also pass the fatigue criteria’s put by BSK99.

In Table 9-1 and Figure 9-2 the parameters and the results for each loading case is presented. The parameters are chosen so that the results are conservative, i.e. minimum number of sheet metal supports, and minimum thicknesses of casing and the guide rings. The linear behaviour of the materials is incorrectly used even after yielding, but the main conclusion is that no buckling is presented before yielding. The curves shown in Figure 9-2 represent the buckling case and the lines represent when yielding occur.

Table 9-1. *Parameters used when analyzing buckling.*

Nr	Casing diameter (mm)	Number of sheet metal supports	Sheet metal support thickness	Top guide ring thickness	Bottom guide ring thickness
1	D-500	12	8 mm	10 mm	20 mm
2	D-750	12	8 mm	10 mm	20 mm
3	D-1000	12	8 mm	10 mm	20 mm
4	D-1250	14	8 mm	10 mm	20 mm
5	D-1500	18	8 mm	10 mm	20 mm
6	D-1750	20	8 mm	10 mm	20 mm
7	D-2000	22	8 mm	10 mm	20 mm

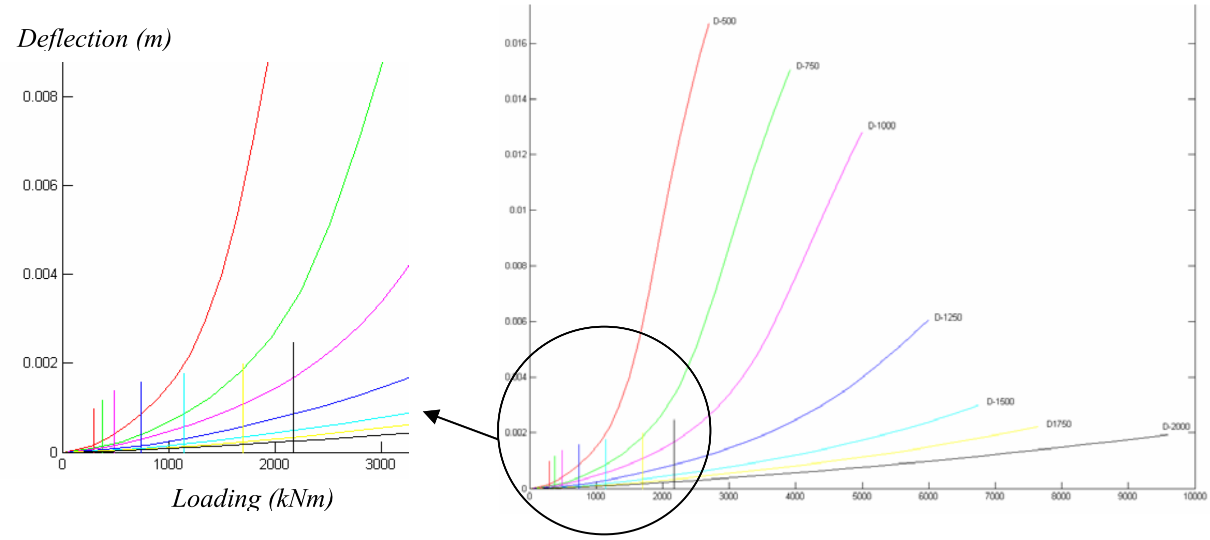

Figure 9-2. *Yielding occurs before buckling.*

10 Strength analysis

When dimensioning, both the yield criterion and the fatigue criterion must be fulfilled for every part of the structure. It must also be investigated which of the criteria that it met first. This is used as the overall loading criterion as regards failure.

As shown in Figure 1-2, there are three different wind exposure types but only two are actually needed to be considered when dimensioning. The loading due to the static wind load must, in fact, not be considered at all, due to the fact that the forces are higher when the chimney is exposed to wind gust, and static loading is, therefore, included when evaluating this kind of loading. This may be seen in Table 3-4. The wind gust and the vortex shedding are therefore considered, only.

In this chapter, a reformulation of the theory is first made, which gives benefits when analyzing the models. Then a stress analysis is performed for each part in order to get a feeling for the behaviour of the models. Finally, a discussion is held over how the parts interact.

10.1 Theoretical considerations

Due to the combination of loadings, the Palmgren-Miner criteria in equation (5.6) was applied, giving

$$\frac{n_{windgust}}{n_{t,windgust}} + \frac{n_{vortexshedding}}{n_{t,vortexshedding}} = 1.0$$

The number of cycles was, as mentioned, obtained from the wind exposure analysis, leaving the number of allowed cycles before break to be calculated from

$$\frac{60000}{n_{t,windgust}} + \frac{10^7}{n_{t,vortexshedding}} = 1.0 \qquad (10.1)$$

The allowed number of cycles could be calculated from the curves in Figure 5-1 which gives

$$f_{rk} = C\left(\frac{2\cdot 10^6}{n_{t,windgust}}\right)^{\frac{1}{3}} \quad \Rightarrow \quad n_{t,windgust} = 2\cdot 10^6\left(\frac{C}{f_{rk}}\right)^3 \qquad (10.2)$$

$$f_{rk} = 0.885\cdot C\left(\frac{2\cdot 10^6}{n_{t,vortexshedding}}\right)^{\frac{1}{5}} \quad \Rightarrow \quad n_{t,vortexshedding} = 2\cdot 10^6\left(\frac{0.885\cdot C}{f_{rk}}\right)^5 \qquad (10.3)$$

Further, the parameter f_{rk} may be replaced by a reformulation of (5.3) and (5.5) giving

$$f_{rk} = \sigma_{rd} 1.1\, \gamma_n$$

The only unknown is the stress width σ_{rd}. It may easily be realized that the larger the applied moment, the higher stress width. The relation is in fact linear due to the linearity of the problem when no yielding occurs. The ratio parameter *k,* i.e. stress width vs. the applied moment, is actually the same for both the loading in terms of the wind gust and for the loading in terms of the vortex shedding and will, therefore, be expresses as

$$\sigma_{rd,windgust} = k \cdot M_{windgust}$$
$$\sigma_{rd,vortexshedding} = k \cdot M_{vortex\ shedding}$$

Insertion into (10.2) and (10.3) gives

$$n_{t,windgust} = 2 \cdot 10^6 \left(\frac{C}{k \cdot M_{windgust} \cdot 1.1 \cdot \gamma_n} \right)^3$$
$$n_{t,vortexshedding} = 2 \cdot 10^6 \left(\frac{0.885 \cdot C}{k \cdot M_{vortex\ shedding} \cdot 1.1 \cdot \gamma_n} \right)^5$$

Finally insertion into the Palmgren-Miner criterion, (10.1) gives

$$\left(\frac{60000}{2 \cdot 10^6 \left(\frac{C}{k \cdot M_{windgust} \cdot 1.1 \cdot \gamma_n} \right)^3} \right) + \left(\frac{10^7}{2 \cdot 10^6 \left(\frac{C}{k \cdot M_{vortex\ sheeding} \cdot 1.1 \cdot \gamma_n} \right)^5} \right) = 1.0 \qquad (10.4)$$

The major benefit of approaching the problem this way is that only the *k* parameter needs to be obtained from an analysis of each part. By knowing *k*, equation (10.4) can be plotted and give the maximum moments allowed, see Figure 10-1.

Another benefit is that the parameter k also holds even if other number of cycles would be obtained from the wind exposure analysis. The expressions in this chapter must, however, be reformulated so that they hold for the new inputs.

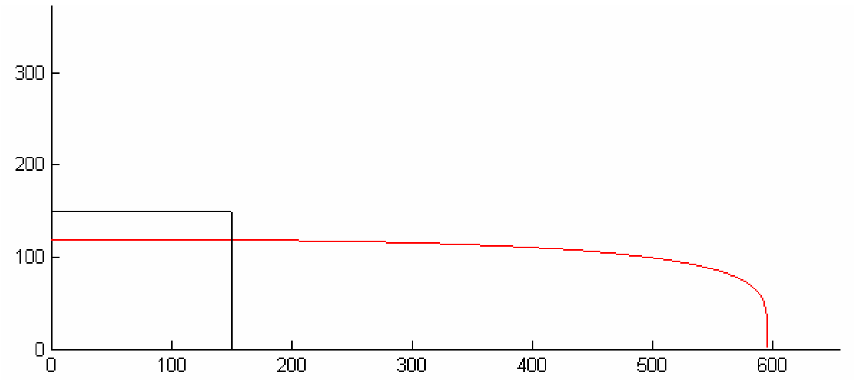

Figure 10-1. *Allowed moments (kNm) for windgust (x-axis) and vortex shedding (y-axis).*

The asymptotes of the curve are actually the moments allowed if the loading would not have been combined.

The second criterion is the yield criterion. If yielding occurs before the above calculated maximum moments are reached, a reduction must be performed leaving the shaded area (the box) in Figure 10-1 as the allowed loading range.

10.2 Analysis of the stresses

The analysis is performed on the section parts that are loaded the most. Those are, not surprising, the parts that are deformed the most, i.e. the parts that are in the direction of the shear force. The maximum principal stresses in the different parts are found at the tensioned side, and marked red in Figure 10-2. The minimum principal stresses are found at the compressed side, and marked blue in Figure 10-2.

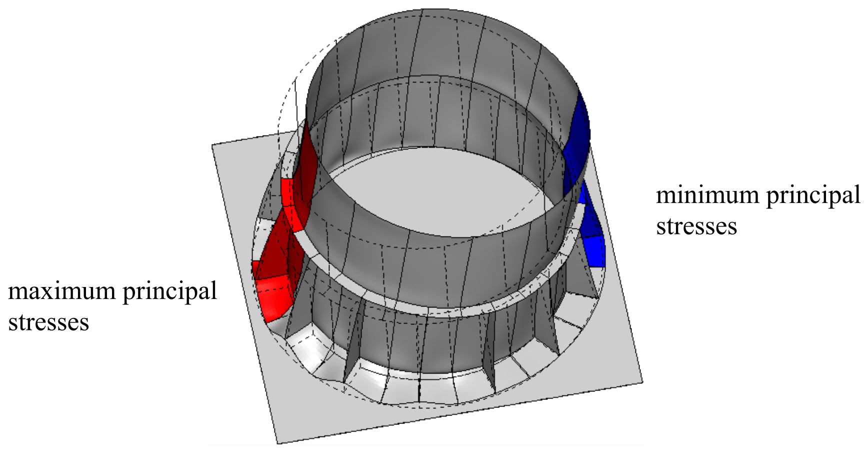

Figure 10-2. *The parts that are loaded the most and further investigated.*

Even though shell elements are used it is possible to evaluate the stresses on both sides of the sheets. The parameter k is calculated at the point of, and at the side on, where the stress width is the highest.

10.2.1 The Casing

Even though the thickness of the casing was dimensioned in the wind exposure analysis and should maintain its strength, the stress width is studied here. The response from the FE-analysis of the casing is shown in Figure 10-3.

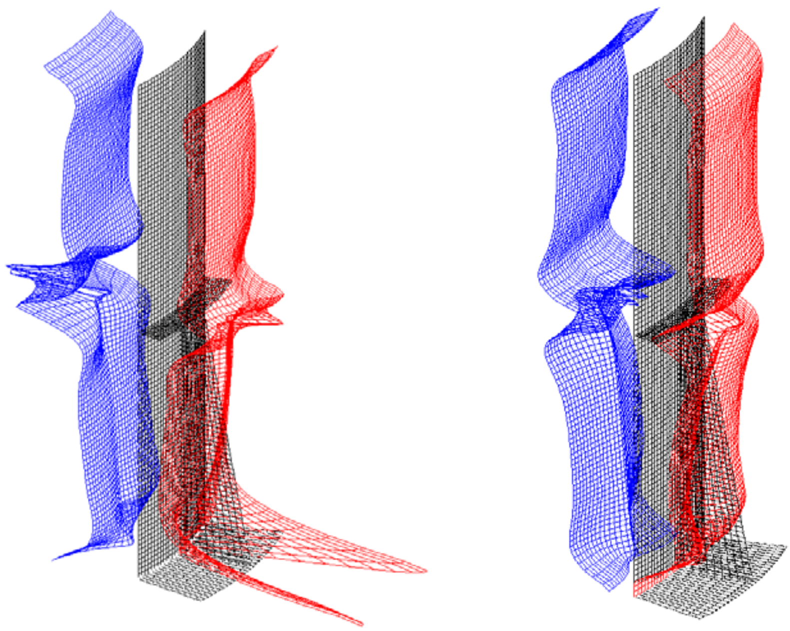

Figure 10-3. *The stress width variation on the inside (left) and the outside (right) of the casing, where red represents the maximum principal stress, blue represents the minimum principal stress and black represents the undeformed state.*

As a matter a fact the result rather is astonishing. It might be seen that the stresses are high in the regions where the guide rings and the sheet metal supports are welded to the casing. However, a more detailed FE-analysis must be performed to evaluate whether singularities are affecting the stresses in these areas. Stress increases also appear at the top of the modelled casing, but here is it no doubt that this may be neglected due to that it is a result of the constraining.

What is astonishing for the casing is that the axial stress above the top guide ring is approximately the same as the evaluated principal stresses due to the simple loading, and, actually, approximately the same as the stresses determined by the Euler-Bernoulli beam theory during the phase of verification of the model.

As expected the stresses below the top guide ring are decreasing, actually due to the same phenomenon that was seen in the phase of verification.

In this master's thesis the parameter *k* for the casing is calculated above the top guide ring in the area that previously was discussed, even though larger stress widths could be obtained at other locations of the casing. This is due to the fact that the casing already is fulfilling the dimensioning criteria's from the wind exposure analysis.

10.2.2 Sheet metal supports

The stress response of the sheet metal supports are shown in Figure 10-4. It might be seen that there is no difference in stresses between the sides of the part. This is not surprising due to the symmetry of the construction. The stress width is almost constant through the height. Therefore, an evaluation of where the stress width should be measured always should be undertaken, in order to determine the *k* parameter.

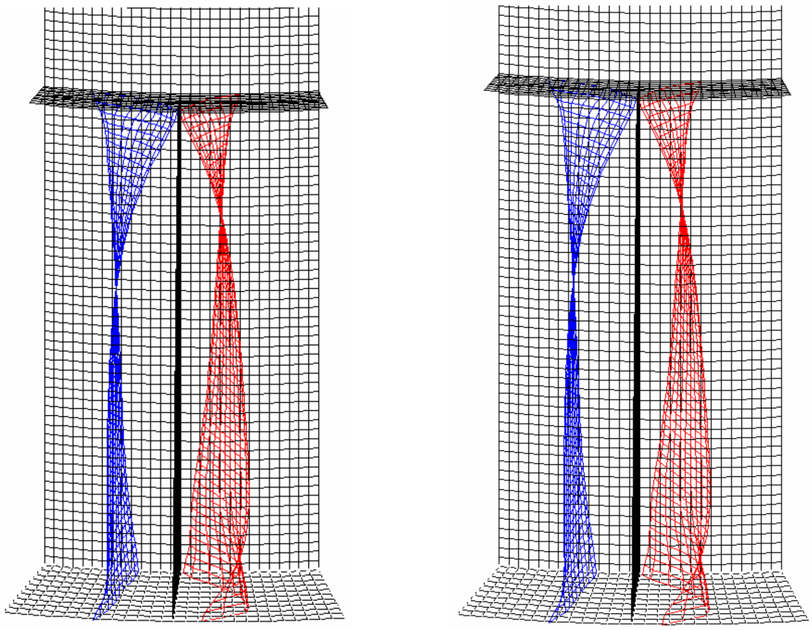

Figure 10-4. *The stress width variation on the left and right side of the sheet metal support, where red represents the maximum principal stress, blue represents the minimum principal stress and black represents the undeformed state.*

10.2.3 Bottom guide ring

The stress response of the bottom guide ring is shown in Figure 10-5. It is not surprising that the stresses on the compressed side are approximately zero due to the inability of the bottom guide ring to deform on this side when pressured against the rigid plate. On the other side it is, however, more problematic. The modelling of the bolt as wires leads to singularities, and, therefore, should a more detailed FE-analysis be performed in order to investigate the stresses here. The assumption is though performed here, assuming that the response around the bolt would, approximately, be the same as the response close to the sheet metal support. Here are the stresses reliable and, therefore, the stress width is measured close to the sheet metal support when evaluating the *k* parameter.

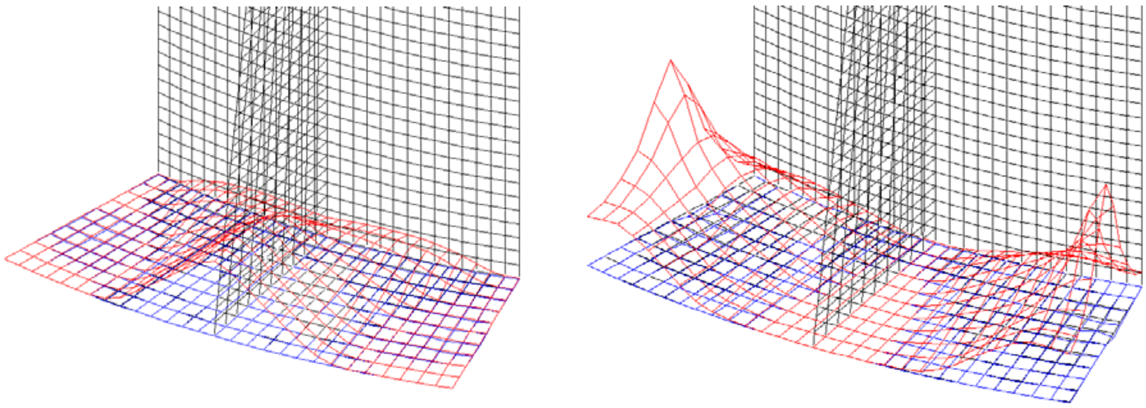

Figure 10-5. *The stress width variation on the top and bottom side of the bottom guide ring, where red represents the maximum principal stress, blue represents the minimum principal stress and black represents the undeformed state.*

10.2.4 Top guide ring

The response of the top guide ring is the most difficult to intuitively say something about due to that the deformation is not easy to imagine and that no analytical calculations applies to the problem. Therefore the results from the FE-analysis are relied upon and presented in Figure 10-6.

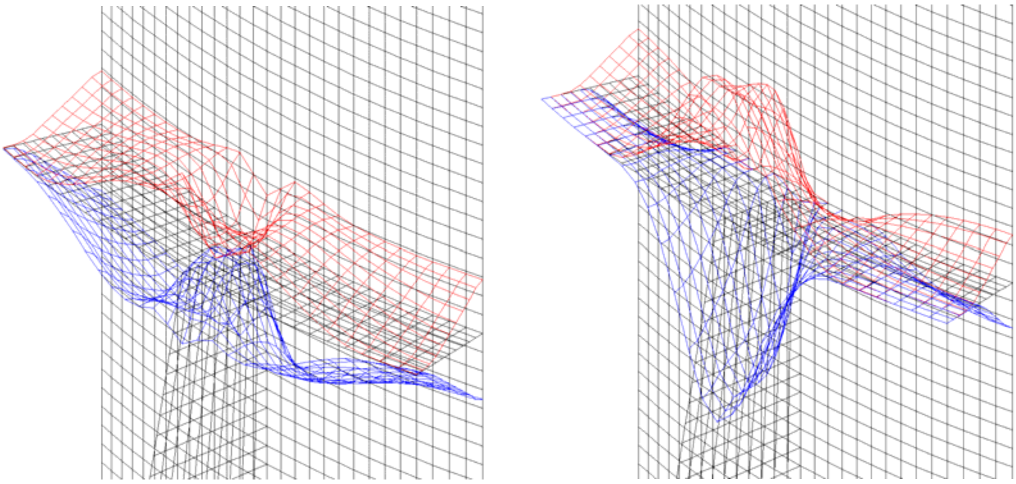

Figure 10-6. *The stress width variation on the top and bottom side of the top guide ring, where red represents the maximum principal stress, blue represents the minimum principal stress and black represents the undeformed state.*

The analysis shows that the stress width of the top guide ring is highest either close to the weld between the guide ring and the casing, or between the guide ring and the sheet metal support. The *k* parameter is therefore evaluated at these positions.

10.3 All loadings combined

All parts will of course not have the same *k* parameter value. But it is easy to realize that the part with the highest *k* parameter value is the one which limits the use of the structure with respect to fatigue. In the same way is the part which reaches yielding first limiting the moments that are possible to apply.

For the structure recently analyzed, the principal stresses and maximum *k* values for the different parts are given in Table 10-1. The yielding is extrapolated from knowing the principal stresses and the measured momentum. The result of the Palmgren-Miner criterion for every part is given in Figure 10-7.

Table 10-1. *The stress width parameter k with the calculated yielding of every part.*

Part	Maximum principal stress	Minimum principal stress	Measured at momentum	k	Yielding
Casing	71	-110	630 kNm	287	1609 kNm
Top guide ring	51	-70	630 kNm	192	2529 kNm
Bottom guide ring	239	0	630 kNm	379	741 kNm
Sheet metal support	73	-117	630 kNm	302	1513 kNm

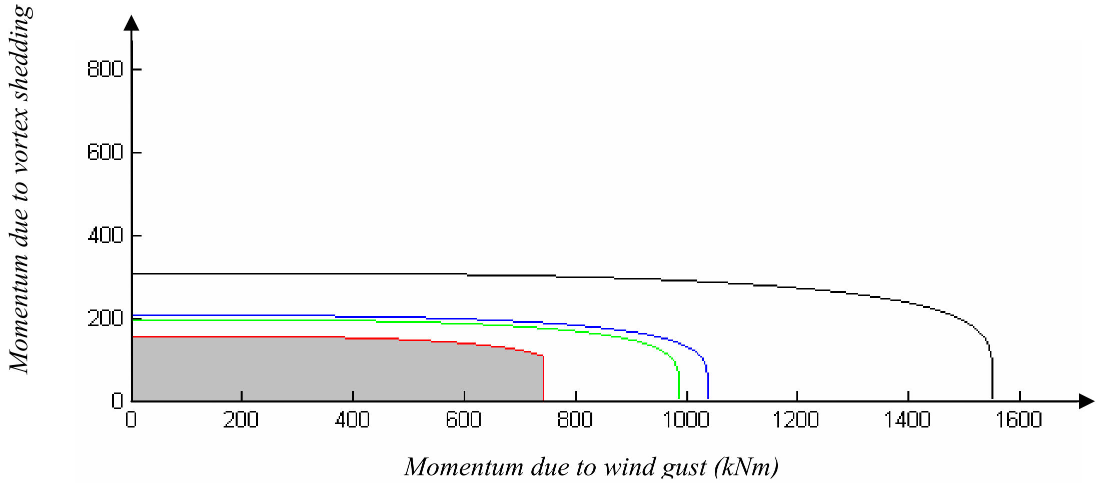

Figure 10-7. *The dimensioning criteria for the sheet metal supports, guide rings and casing.*

As seen, the bottom guide ring is loaded the most and is, therefore, setting the dimensioning criteria for this chimney. It is not difficult to realize that using more sheet metal supports results in lower *k* parameter values and yielding moments for all parts except of the casing. Therefore is it only necessary to analyze every chimney until the casing sets the dimensioning criterion, both for the *k* parameter and for the yielding.

10.4 Results

10.4.1 D-500 mm

For the chimney with a casing diameter 500 mm, the principal stresses and maximum k values for different parts analyzed are shown in Table 10-2. The yielding is extrapolated from knowing the principal stresses and the measured moment. The values marked yellow in Table 10-2 show the parts of the chimney that reach yielding first, and red values denote when the casing is setting the limit. The result of the Palmgren-Miner criterion for the most exposed part is given in Figure 10-8, with case numbers according to Table 10-2.

Table 10-2. *The stress width parameter k with the calculated yielding of the most exposed part.*

	Geometry (number; mm)		Sheet M S		Bottom Guide Ring		Top Guide Ring		Casing			k parameter				Part	Yield	kmax
Nr	Sheet metal supports	Casing thickness	Max Princ	Min Princ	Max Princ	Min Princ	Max Princ	Min Princ	Max Princ	Min Princ	Measured at torque (kNm)	Sheet M S	Bottom guide ring	Top guide ring	Casing		(kNm)	
1	12	6	170	-205	225	0	56	-59	240	-252	270	1 389	833	426	1 822	Casing	301	1 822
2	16	6	178	-201	135	0	66	-69	265	-277	300	1 263	450	450	1 807	Casing	304	1 807
3	20	6	170	-184	127	0	67	-70	267	-276	300	1 180	423	457	1 810	Casing	305	1 810
4	12	8	146	-182	239	0	61	-72	188	-200	297	1 104	805	448	1 306	B G R	349	1 306
5	16	8	154	-178	143	0	73	-81	214	-228	330	1 006	433	467	1 339	Casing	407	1 339
6	20	8	148	-164	135	0	73	-80	216	-228	330	945	409	464	1 345	Casing	407	1 345
7	12	10	117	-151	225	0	60	-75	146	-159	288	931	781	469	1 059	B G R	360	1 059
8	16	10	141	-167	153	0	91	-105	185	-197	360	856	425	544	1 061	Casing	514	1 061
9	20	10	136	-154	88	0	92	-104	184	-196	360	806	244	544	1 056	Casing	516	1 056
10	12	12	150	-109	209	0	70	-91	113	-126	273	949	766	590	875	B G R	367	949
11	16	12	196	-110	162	0	104	-123	165	-178	390	785	415	582	879	Sheet M S	559	879
12	20	12	140	-150	89	0	105	-121	166	-177	390	744	228	579	879	Casing	619	879

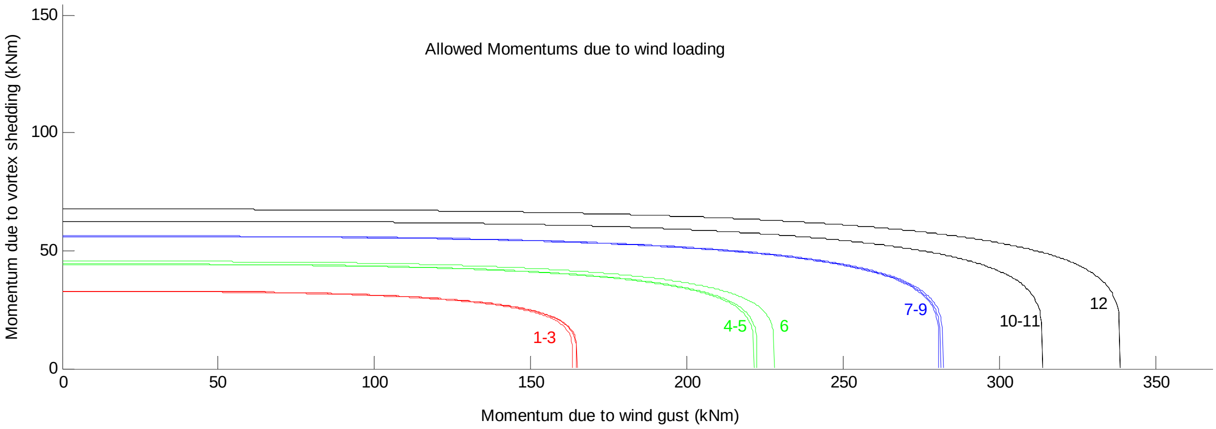

Figure 10-8. *The dimensioning criteria for the most exposed part in the structure.*

10.4.2 D-750 mm

For the chimney with a casing diameter 750 mm, the principal stresses and maximum *k* values for different parts analyzed are shown in Table 10-3. The yielding is extrapolated from knowing the principal stresses and the measured moment. The values marked yellow in Table 10-3 show the parts of the chimney that reach yielding first, and red values denote when the casing is setting the limit. The result of the Palmgren-Miner criterion for the most exposed part is given in Figure 10-9, with case numbers according to Table 10-3.

Table 10-3. *The stress width parameter k with the calculated yielding of the most exposed part.*

	Geometry (number; mm)		Sheet M S		Bottom Guide Ring		Top Guide Ring		Casing			k parameter				Part	Yield	kmax
Nr	Sheet metal supports	Casing thickness	Max Princ	Min Princ	Max Princ	Min Princ	Max Princ	Min Princ	Max Princ	Min Princ	Measured at torque (kNm)	Sheet M S	Bottom guide ring	Top guide ring	Casing			
1	12	6	78	-104	187	0	77	-11	92	-110	255	714	733	345	792	B G R	383	792
2	16	6	142	-170	212	0	56	-70	191	-213	500	624	424	252	808	Casing	660	808
3	20	6	135	-154	143	0	71	-83	193	-211	500	578	286	308	808	Casing	666	808
4	24	6	129	-143	97	0	58	-67	195	-210	500	544	194	250	810	Casing	669	810
5	12	8	111	-100	223	0	25	-39	85	-105	318	664	701	201	597	B G R	401	701
6	16	8	154	-123	219	0	48	-64	149	-171	530	523	413	211	604	B G R	680	604
7	20	8	112	-133	146	0	48	-60	151	-169	530	462	275	204	604	Casing	881	604
8	24	8	97	-112	90	0	45	-53	136	-150	477	438	189	205	600	Casing	894	600
9	12	10	110	-98	224	0	27	-45	71	-91	336	619	667	214	482	B G R	422	667
10	16	10	140	-107	199	0	46	-72	110	-132	504	490	395	234	480	B G R	712	490
11	20	10	157	-84	150	0	51	-76	124	-143	560	430	268	227	477	Sheet M S	1 002	477
12	24	10	96	-113	102	0	60	-74	125	-141	560	373	182	239	475	Casing	1 116	475
13	12	12	108	-95	221	0	34	-60	60	-80	350	580	631	269	400	B G R	445	631
14	16	12	142	-105	206	0	57	-83	94	-114	531	465	388	264	392	B G R	724	465
15	20	12	170	-99	173	0	74	-98	121	-141	665	405	260	259	394	B G R	1 080	405
16	24	12	136	-75	104	0	67	-85	109	-125	590	358	176	258	397	Sheet M S	1 219	397
17	28	12	187	-87	143	0	93	-113	150	-167	800	343	179	258	396	Sheet M S	1 202	396
18	32	12	97	-132	74	0	69	-97	131	-189	800	286	93	208	400	Casing	1 189	400

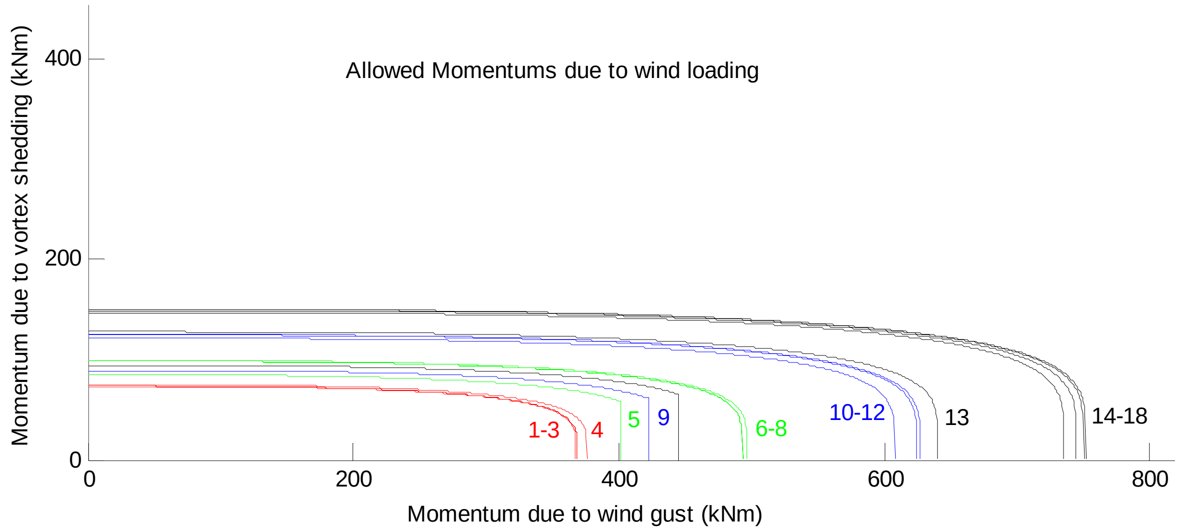

Figure 10-9. *The dimensioning criteria for the most exposed part in the structure.*

10.4.3 D-1000 mm

For the chimney with a casing diameter 1000 mm, the principal stresses and maximum *k* values for different parts analyzed are shown in Table 10-4. The yielding is extrapolated from knowing the principal stresses and the measured moment. The values marked yellow in Table 10-4 show the parts of the chimney that reach yielding first, and red values denote when the casing is setting the limit. The result of the Palmgren-Miner criterion for the most exposed part is given in Figure 10-10, with case numbers according to Table 10-4.

Table 10-4. *The stress width parameter k with the calculated yielding of the most exposed part.*

	Geometry (number; mm)		Sheet M S		Bottom Guide Ring		Top Guide Ring		Casing			k parameter				Part	Yield	kmax
Nr	Sheet metal supports	Casing thickness	Max Princ	Min Princ	Max Princ	Min Princ	Max Princ	Min Princ	Max Princ	Min Princ	Measured at torque (Nm)	Sheet M S	Bottom guide ring	Top guide ring	Casing		(kNm)	
1	12	6	102	-101	242	0	50	-73	81	-116	420	483	576	293	469	B G R	488	576
2	16	6	128	-99	232	0	53	-62	114	-144	560	405	414	205	461	B G R	678	461
3	20	6	111	-135	191	0	53	-58	147	-175	700	351	273	159	460	B G R	1 030	460
4	24	6	106	-124	138	0	50	-55	150	-147	700	329	197	150	424	Casing	1 311	424
5	12	8	98	-97	237	0	38	-60	60	-91	444	439	534	221	340	B G R	526	534
6	16	8	126	-95	232	0	42	-52	86	-115	592	373	392	159	340	B G R	717	392
7	20	8	145	-106	212	0	48	-53	124	-154	810	310	262	125	343	B G R	1 074	343
8	24	8	87	-107	140	0	39	-44	115	-140	740	262	189	112	345	Casing	1 485	345
9	12	10	95	-94	232	0	31	-51	49	-81	468	404	496	175	278	B G R	567	496
10	16	10	125	-92	233	0	34	-44	70	-100	624	348	373	125	272	B G R	753	373
11	20	10	137	-84	187	0	37	-52	88	-115	750	295	249	119	271	B G R	1 127	295
12	24	10	131	-75	143	0	39	-52	94	-118	780	264	183	117	272	B G R	1 533	272
13	28	10	130	-66	109	0	47	-61	97	-119	800	245	136	135	270	Casing	1 729	270
14	12	12	74	-75	180	0	20	-46	33	-59	410	363	439	161	224	B G R	640	439
15	16	12	125	-90	232	0	37	-64	59	-88	656	328	354	154	224	B G R	795	354
16	20	12	136	-91	198	0	49	-74	79	-107	820	277	241	150	227	B G R	1 164	277
17	24	12	130	-74	146	0	51	-70	80	-104	820	249	178	148	224	B G R	1 578	249
18	28	12	100	-51	84	0	41	-55	63	-83	651	232	129	147	224	Sheet M S	1 829	232
19	32	12	121	-58	79	0	53	-67	82	-102	820	218	96	146	224	Sheet M S	1 904	224

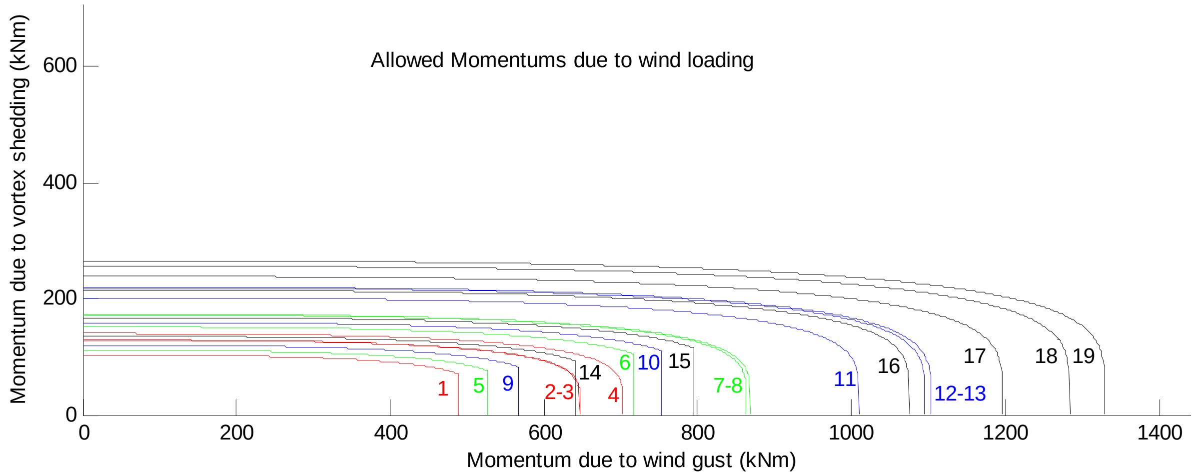

Figure 10-10. *The dimensioning criteria for the most exposed part in the structure.*

10.4.4 D-1250 mm

For the chimney with a casing diameter 1250 mm, the principal stresses and maximum *k* values for different parts analyzed are shown in Table 10-5. The yielding is extrapolated from knowing the principal stresses and the measured moment. The values marked yellow in Table 10-5 show the parts of the chimney that reach yielding first, and red values denote when the casing is setting the limit. The result of the Palmgren-Miner criterion for the most exposed part is given in Figure 10-11, with case numbers according to Table 10-5.

Table 10-5. *The stress width parameter k with the calculated yielding of the most exposed part.*

	Geometry (number; mm)		Sheet M S		Bottom Guide Ring		Top Guide Ring		Casing			k parameter				Part	Yield	kmax
Nr	Sheet metal supports	Casing thickness	Max Princ	Min Princ	Max Princ	Min Princ	Max Princ	Min Princ	Max Princ	Min Princ	Measured at torque (Nm)	Sheet M S	Bottom guide ring	Top guide ring	Casing		(kNm)	
1	14	6	71	-110	239	0	51	-70	73	-117	630	287	379	192	302	B G R	741	379
2	18	6	120	-91	229	0	53	-60	95	-134	765	276	299	148	299	B G R	939	299
3	22	6	109	-79	170	0	47	-49	103	-136	800	235	213	120	299	B G R	1 322	299
4	26	6	97	-119	160	0	52	-56	133	-165	1 000	216	160	108	298	Casing	1 703	298
5	14	8	99	-96	219	0	34	-49	59	-101	705	277	311	118	227	B G R	905	311
6	18	8	118	-89	229	0	42	-49	71	-109	818	253	280	111	220	B G R	1 004	280
7	22	8	127	-89	200	0	44	-47	91	-127	984	220	203	92	222	B G R	1 383	222
8	26	8	124	-86	168	0	43	-45	105	-138	1 100	191	153	80	221	B G R	1 840	221
9	30	8	129	-70	130	0	37	-45	106	-135	1 100	181	118	75	219	Casing	2 290	219
10	14	10	84	-81	206	0	27	-42	38	-74	640	258	322	108	175	B G R	873	322
11	18	10	104	74	202	0	29	-47	50	-80	740	41	273	103	176	B G R	1 029	273
12	22	10	140	-93	221	0	37	-53	80	-116	1 133	206	195	79	173	B G R	1 441	206
13	26	10	130	-86	176	0	39	-53	89	-121	1 200	180	147	77	175	B G R	1 916	180
14	30	10	28	-22	29	0	10	-16	19	-37	323	155	90	80	173	Casing	2 453	173
15	14	12	70	-69	169	0	18	-44	27	-61	601	231	281	103	146	B G R	999	281
16	18	12	122	-88	237	0	34	-62	50	-86	951	221	249	101	143	B G R	1 128	249
17	22	12	114	-74	176	0	37	-59	55	-86	975	193	181	98	145	B G R	1 557	193
18	26	12	144	-83	186	0	52	-74	77	-110	1 300	175	143	97	144	B G R	1 964	175
19	30	12	141	-72	144	0	53	-72	78	-107	1 300	164	111	96	142	B G R	2 537	164

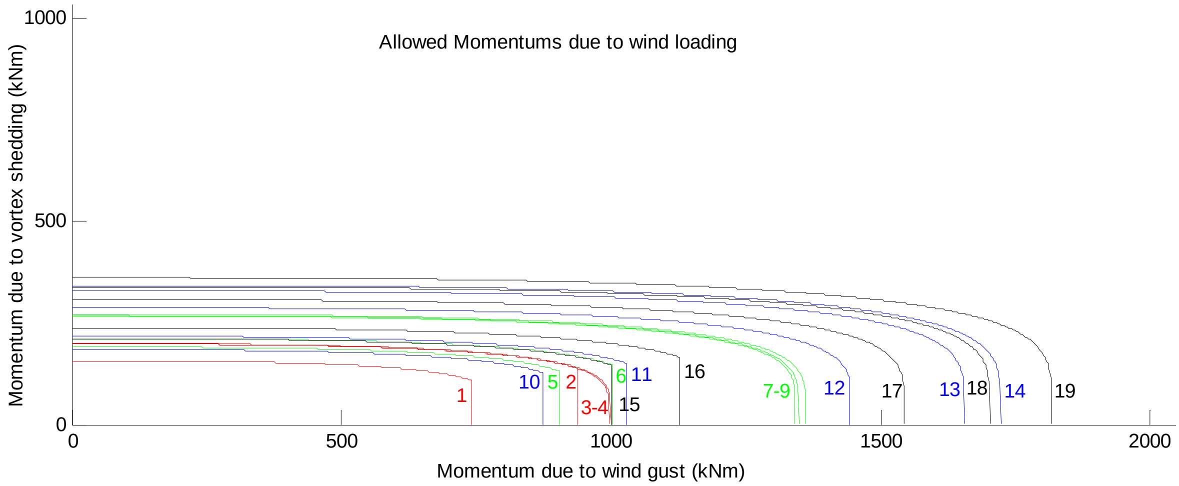

Figure 10-11. *The dimensioning criteria for the most exposed part in the structure.*

10.4.5 D-1500 mm

For the chimney with a casing diameter 1500 mm, the principal stresses and maximum *k* values for different parts analyzed are shown in Table 10-6. The yielding is extrapolated from knowing the principal stresses and the measured momentum. The values marked yellow in Table 10-6 show the parts of the chimney that reach yielding first, red values denote when the casing is setting the limit and blue values represent when further analyses are needed. The result of the Palmgren-Miner criterion for the most exposed part is given in Figure 10-12, with case numbers according to Table 10-6.

Table 10-6. *The stress width parameter k with the calculated yielding of the most exposed part.*

	Geometry (number; mm)		Sheet M S		Bottom Guide Ring		Top Guide Ring		Casing			k parameter				Part	Yield	kmax
Nr	Sheet metal supports	Casing thickness	Max Princ	Min Princ	Max Princ	Min Princ	Max Princ	Min Princ	Max Princ	Min Princ	Measured at torque (Nm)	Sheet M S	Bottom guide ring	Top guide ring	Casing			
1	18	6	95	-79	206	0	46	-57	66	-112	840	207	245	123	212	B G R	1 146	245
2	22	6	108	-78	197	0	51	-54	83	-125	1 000	186	197	105	208	Casing	1 426	208
3	26	6	95	-67	146	0	44	-45	86	-123	1 000	162	146	89	209	Casing	1 925	209
4	30	6	65	-85	113	0	40	-39	88	-120	1 000	150	113	79	208	Casing	2 342	208
5	18	8	94	-78	206	0	36	-47	50	-94	914	188	225	91	158	B G R	1 247	225
6	22	8	94	-71	157	0	32	-33	58	-96	1 000	165	157	65	154	B G R	1 790	165
7	26	8	98	-68	151	0	36	-38	67	-103	1 100	151	137	67	155	Casing	2 047	155
8	30	8	88	-60	118	0	34	-34	68	-101	1 100	135	107	62	154	Casing	2 619	154
9	34	8	85	-53	73	0	27	-32	70	-99	1 100	125	66	54	154	Casing	3 122	154
10	18	10	94	-79	209	0	29	-39	40	-83	1 000	173	209	68	123	B G R	1 344	209
11	22	10	114	-79	208	0	26	-41	52	-93	1 200	161	173	56	121	B G R	1 621	173
12	26	10	102	-68	156	0	31	-40	55	-90	1 200	142	130	59	121	Sheet M S	2 162	142
13	30	10	91	-61	94	0	32	-39	56	-88	1 200	127	78	59	120	Sheet M S	3 587	127
14	34	10																
15	18	12	94	-78	206	0	25	-52	33	-74	1 073	160	192	72	100	B G R	1 464	192
16	22	12	103	-79	212	0	33	-58	45	-85	1 300	140	163	70	100	B G R	1 723	163
17	26	12	106	-68	161	0	35	-55	47	-82	1 300	134	124	69	99	B G R	2 269	134
18	30	12	95	-61	118	0	36	-53	48	-79	1 300	120	91	68	98	B G R	3 096	120
19	34	12	92	-54	80	0	26	-34	49	-78	1 300	112	62	46	98	Sheet M S	3 971	112
20	38	12	87	-50	49	0	27	-35	50	-77	1 300	105	38	48	98	Sheet M S	4 199	105

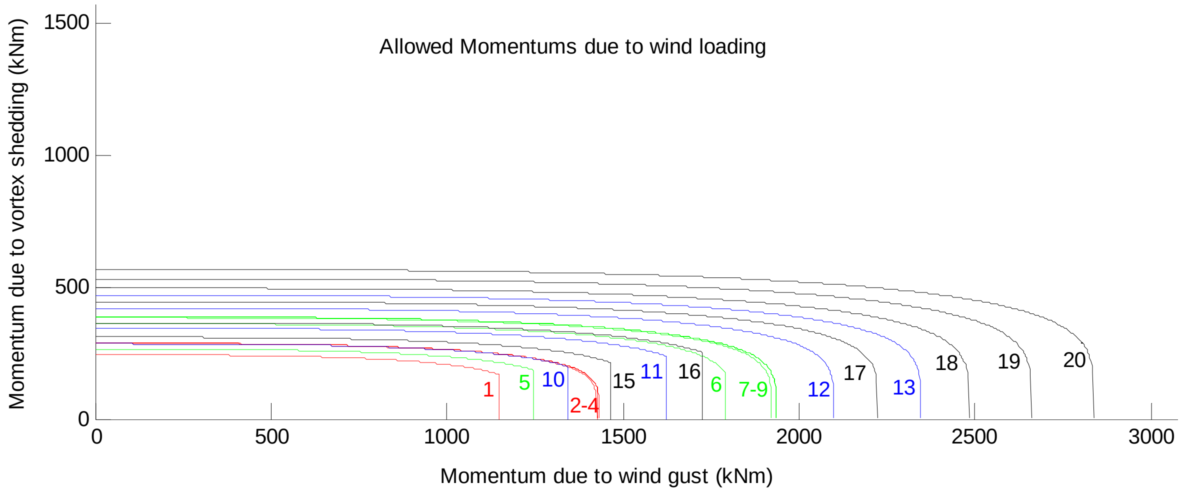

Figure 10-12. *The dimensioning criteria for the most exposed part in the structure.*

10.4.6 D-1750 mm

For the chimney with a casing diameter 1750 mm, the principal stresses and maximum k values for different parts analyzed are shown in Table 10-7. The yielding is extrapolated from knowing the principal stresses and the measured moment. The values marked yellow in Table 10-7 show the parts of the chimney that reach yielding first, red values denote when the casing is setting the limit and blue values represent when further analyses are needed. The result of the Palmgren-Miner criterion for the most exposed part is given in Figure 10-13, with case numbers according to Table 10-7.

Table 10-7. *The stress width parameter k with the calculated yielding of the most exposed part.*

	Geometry (number; mm)		Sheet M S		Bottom Guide Ring		Top Guide Ring		Casing			k parameter				Part	Yield	kmax
Nr	Sheet metal supports	Casing thickness	Max Princ	Min Princ	Max Princ	Min Princ	Max Princ	Min Princ	Max Princ	Min Princ	Measured at torque (Nm)	Sheet M S	Bottom guide ring	Top guide ring	Casing		(kNm)	
1	20	6	102	-86	207	0	47	-58	70	-124	1 250	150	166	84	155	B G R	1 697	166
2	24	6	101	-73	189	0	51	-54	73	-121	1 250	139	151	84	155	B G R	1 858	155
3	28	6	93	-64	151	0	46	-47	75	-118	1 250	126	121	74	154	B G R	2 326	154
4	32	6	82	-57	98	0	37	-36	77	-114	1 250	111	78	58	153	Casing	3 081	153
5	36	6	78	-52	73	0	32	-32	79	-113	1 250	104	58	51	154	Casing	3 108	154
6	20	8	103	-85	231	0	42	-53	50	-103	1 330	141	174	71	115	B G R	1 618	174
7	24	8	98	-72	184	0	39	-44	53	-98	1 330	128	138	62	114	B G R	2 031	138
8	28	8	92	-63	150	0	36	-39	55	-95	1 330	117	113	56	113	B G R	2 492	117
9	32	8	82	-57	120	0	34	-35	57	-93	1 330	105	90	52	113	B G R	3 114	113
10	36																	
11	20	10	99	-83	223	0	33	-43	39	-90	1 410	129	158	54	91	B G R	1 777	158
12	24	10	97	-71	180	0	31	-36	41	-84	1 410	119	128	48	89	Casing	2 201	128
13	28	10	91	-62	147	0	27	-36	43	-82	1 410	109	104	45	89	B G R	2 695	109
14	32	10	82	-56	119	0	28	-35	44	-79	1 410	98	84	45	87	B G R	3 329	98
15	36																	
16	20	12	97	-81	214	0	25	-54	31	-79	1 490	119	144	53	74	B G R	1 956	144
17	24	12	95	-69	176	0	27	-51	33	-75	1 490	110	118	52	72	B G R	2 379	118
18	28	12	90	-61	144	0	29	-49	35	-72	1 490	101	97	52	72	B G R	2 908	101
19	32	12	81	-55	116	0	30	-47	36	-70	1 490	91	78	52	71	B G R	3 609	91
20	36	12	70	-47	66	0	21	-30	34	-65	1 400	84	47	36	71	Sheet M S	5 620	84

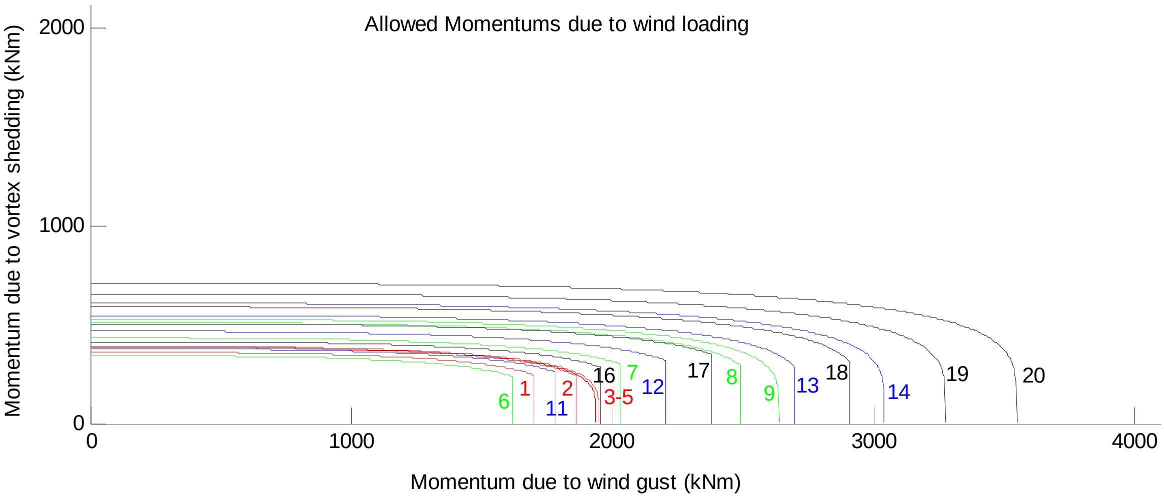

Figure 10-13. *The dimensioning criteria for the most exposed part in the structure.*

10.4.7 D-2000 mm

For the chimney with a casing diameter 2000 mm, the principal stresses and maximum *k* values for different parts analyzed are shown in Table 10-8. The yielding is extrapolated from knowing the principal stresses and the measured moment. The values marked yellow in Table 10-8 show the parts of the chimney that reach yielding first, red values denote when the casing is setting the limit and blue values represent when further analyses are needed. The result of the Palmgren-Miner criterion for the most exposed part is given in Figure 10-14, with case numbers according to Table 10-8.

Table 10-8. *The stress width parameter k with the calculated yielding of the most exposed part.*

	Geometry (number; mm)		Sheet M S		Bottom Guide Ring		Top Guide Ring		Casing			k parameter				Part	Yield	kmax
Nr	Sheet metal supports	Casing thickness	Max Princ	Min Princ	Max Princ	Min Princ	Max Princ	Min Princ	Max Princ	Min Princ	Measured at torque (Nm)	Sheet M S	Bottom guide ring	Top guide ring	Casing		(kNm)	
1	22	6	92	-79	194	0	45	-58	61	-119	1 500	114	129	69	120	B G R	2 173	129
2	26	6	36	-38	67	0	17	-26	28	-66	796	93	84	54	118	B G R	3 338	118
3	30	6	82	-61	124	0	39	-41	65	-111	1 500	95	83	53	117	B G R	3 399	117
4	34	6	76	-55	96	0	35	-36	67	-108	1 500	87	64	47	117	Casing	3 903	117
5	38	6	5	-22	8	0	3	-10	7	-34	351	77	23	37	117	Casing	2 901	117
6	22	8	117	-96	249	0	43	-56	57	-120	2 000	107	125	50	89	B G R	2 257	125
7	26	8	78	-64	137	0	27	-35	41	-88	1 500	95	91	41	86	B G R	3 077	95
8	30	8	74	-57	111	0	27	-31	43	-85	1 500	87	74	39	85	B G R	3 797	87
9	34	8	67	-52	86	0	23	-29	45	-86	1 500	79	57	35	87	Casing	4 901	87
10	38	8	65	-48	74	0	24	-26	46	-82	1 500	75	49	33	85	Casing	5 140	85
11	22	10	83	-77	177	0	25	-36	33	-84	1 700	94	104	36	69	B G R	2 699	104
12	26	10	69	-59	120	0	17	-29	29	-72	1 500	85	80	31	67	B G R	3 513	85
13	30	10	73	-56	108	0	19	-30	33	-73	1 600	81	68	31	66	B G R	4 163	81
14	34	10	67	-52	85	0	21	-29	34	-71	1 600	74	53	31	66	B G R	5 289	74
15	38	10	43	-37	48	0	14	-21	24	-55	1 200	67	40	29	66	Casing	6 131	67
16	22	12	94	-83	198	0	18	-37	30	-82	2 000	89	99	28	56	B G R	2 838	99
17	26	12	74	-62	128	0	16	-31	25	-67	1 600	85	80	29	58	B G R	3 513	85
18	30	12	91	-65	134	0	22	-35	33	-74	2 000	78	67	29	54	B G R	4 194	78
19	34	12	84	-59	105	0	23	-34	34	-72	2 000	72	53	29	53	B G R	5 352	72
20	38	12	79	-54	91	0	23	-32	35	-71	2 000	67	46	28	53	B G R	6 176	67
21	42	12																

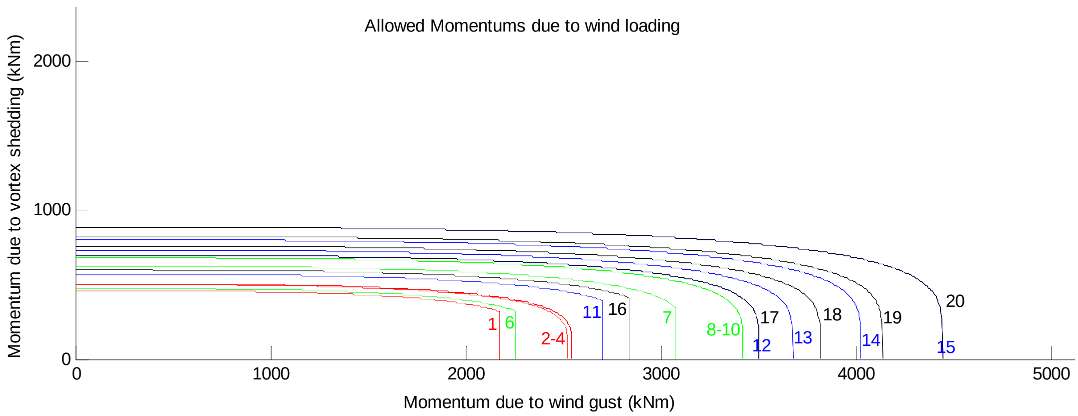

Figure 10-14. *The dimensioning criteria for the most exposed part in the structure.*

11 Conclusions

The main objective of this Master's thesis was to analyze buckling of the sheet metal supports and to create a construction manual to guide the designers at Gullmanders Arking AB.

Many of the geometrical variables were standardized. The sheet metal support could be decreased with 4 mm of thickness from the original thickness of 12 mm. It could be shown that buckling was not an issue, even for this thickness level. Instead, the fatigue criterion was shown to be the dimensioning factor.

Further were the guide rings given constant thicknesses. It could be seen from the strength analysis that the top guide ring never was close to failure, and it was therefore standardized to 10 mm. The bottom guide ring was, however, heavily loaded, and the number of sheet metal supports was of big importance when considering the yielding criterion. The thickness of the bottom guide ring was set to 20 mm.

The way of treating the problem, with the k parameter, makes it easy to analyze whether a structure will maintain its strength when loaded with the loading applied from the wind exposure analysis. The fatigue criterion may easily be reformulated even if the number of cycles would be changed, which makes the solution applicable in all situations.

Before using the results of this Master's thesis an evaluation of the approximations should be performed, showing that the input data from the wind exposure analysis are conservative.

If comparing the dimensions of the chimneys given from the input data with the geometry resulting from the calculations, it may be seen that all chimneys previously were too conservatively built.

12 Future work

As mentioned an evaluation must be performed regarding the effects of the stress intensities in the casing. A further and more detailed investigation must also be performed on the bottom guide ring due to the singularity that appeared from the modelling of the bolts.

The bolts were never evaluated in this master’s thesis and a further investigation must be performed to see whether standardization is possible.

This Master’s thesis might be used as an input for a more detailed investigation regarding optimising the geometry. Depending on the loading situation for each part, an evaluation may be performed to show what optimal k value should be used. For instance is the loading on the casing, sheet metal supports and the top guide ring approximately fully symmetric, and the perfect k value would be the one that the casing has. The loading on the bottom guide ring is not symmetric and, therefore, must an evaluation be performed leading to an optimal k value.

The detailed parts of the chimney are welded together in different ways and, therefore, a welding evaluation was considered to be done in the original objective, aiming at decreasing the measures, if possible. From our analysis it was shown that no improvement were found, perhaps due to the fact that the welds were never modelled (shell element) and, therefore, lower accuracy was obtained. By modelling the welds better the accuracy could be improved, and improvements may be easier to find.

13 References

ABAQUS, version 6.7, Hibbitt, Karlsson & Sorensen, Inc.

Boverket. (Utgåva 2, 1998). Boverkets handbok om Snö- och vindlast (BSV97). ISBN 91-7147-394-7.

Björk, K. (Femte upplagan). Formler och Tabeller för Mekanisk Konstruktion. Institutionen för mekanik och hållfasthetslära, Karl Björks Förlag AB.

Eriksson, Åsa / Lignell, Anna-Maria / Olsson, Claes / Spennare, Hans. (2002). Svetsutvärdering med FEM. Handbok för utmattningsbelastade konstruktioner. Printed by Industrilitteratur AB. ISBN 91-7548-636-9.

Karlebo Handbok (2000), edition 15,Printed in Sweden 2000. ISBN 91-47-01558-6.

Göransson, L. and Åkerlund, S. (Upplaga 3:3, December, 2001). Boverkets handbok om Stålkonstruktioner, BSK99. Printed by Boverket, Byggavdelningen. ISBN 91-7147-527-3.

Olsson, C. (Utgåva 3, 2005). Konstruktionshandbok för svetsade produkter. Printed by Nya Almqvist & Wiksell AB, Uppsala 2005. ISBN 91-7548-677-6.

Ottosen, Niels Saabye and Ljung, Christer (Juni 2003). Hållfasthetslära del 1, Enaxliga tillstånd. Institutionen för hållfatshetslära, Lunds Universitet.

Ottosen, Niels Saabye and Ljung, Christer (Autumn 2003). Strength of Materials and Solid Mechanics, AK 2. Division of Solid Mechanics, Lund University.

Python. http://www.python.org/

Sundström, B. (1998). Handbok och Formelsamling i Hållfasthetslära. Institutionen för hållfasthetslära, KTH, Fingraf AB, Södertälje.